

**TECHNICAL REPORT STANDARD PAGE**

1. Report No. <b>FHWA/LA.08/441</b>		2. Government Accession No.	3. Recipient's Catalog No.
4. Title and Subtitle <b>A Novel Technique For Stiffening Steel Structures</b>		5. Report Date <b>March 2009</b>	
		6. Performing Organization Code	
7. Author(s) <b>Ayman M. Okeil, Ph.D., P.E. Yilmaz Bingol, Ph.D. Md. Rubiat Ferdous</b>		8. Performing Organization Report No.	
9. Performing Organization Name and Address Department of Civil and Environmental Engineering Louisiana State University Baton Rouge, LA 70803		10. Work Unit No.	
		11. Contract or Grant No. <b>LTRC Project Number: 07-4TIRE State Project Number: 736-99-1447</b>	
12. Sponsoring Agency Name and Address <b>Louisiana Department of Transportation and Development P.O. Box 94245 Baton Rouge, LA 70804-9245</b>		13. Type of Report and Period Covered <b>Final Report February 2007 – June 2008</b>	
		14. Sponsoring Agency Code	
15. Supplementary Notes <b>Conducted in Cooperation with the U.S. Department of Transportation, Federal Highway Administration</b>			
<p>16. <b>Abstract</b></p> <p>The use of composite materials for strengthening the ailing infrastructure has been steadily gaining acceptance and market share. One can state that this strengthening technique has become main stream in some applications such as in strengthening of concrete structures. The same cannot be said about steel structures since research on composite strengthening is relatively new. Several challenges face strengthening steel structures using composite materials such as the need for high modulus composites to improve the effectiveness of the strengthening system.</p> <p>In this study, the research team explores a new approach for strengthening steel structures by introducing additional stiffness to buckling prone regions in thin-walled steel structures. The proposed technique relies on improving the <i>out-of-plane</i> stiffness of buckling prone members by bonding pultruded fiber reinforced polymers (FRP) sections as opposed to the commonly used strengthening approach that relies on <i>in-plane</i> FRP contribution. This report presents the results from an experimental investigation where axial tension and beam specimens were tested to explore the feasibility of the proposed technique. Based on the results, one can conclude that this strengthening technique has great potential for altering failure modes by delaying the undesirable instability (buckling) failure mode. Preliminary analyses were also conducted and are presented in the report. Recommendations for future research efforts are made to expand the knowledge base about this yet unexplored strengthening technique.</p>			
17. Key Words Composites, strengthening, steel, adhesives, epoxy, shear failure, buckling, pultruded sections		18. Distribution Statement Unrestricted. This document is available through the National Technical Information Service, Springfield, VA 21161	
19. Security Classification (of this report) N/A	20. Security Classification (of this page) N/A	21. No. of Pages 78	22. Price N/A



# **A Novel Technique for Stiffening Steel Structures**

by

Ayman M. Okeil, Ph.D., PE.  
Assistant Professor

Yilmaz Bingol, Ph.D. Candidate,  
Research Assistant

Md. Rubiat Ferdous, MSCE  
Former Research Assistant

Department of Civil and Environmental Engineering  
3510 Patrick F. Taylor Hall  
Louisiana State University  
Baton Rouge, LA 70803

LTRC Project No. 07-4TIRE  
State Project No. 736-99-1447

conducted for

Louisiana Department of Transportation and Development  
Louisiana Transportation Research Center

The contents of this report reflect the views of the author/principal investigator who is responsible for the facts and the accuracy of the data presented herein. The contents of do not necessarily reflect the views or policies of the Louisiana Department of Transportation and Development or the Louisiana Transportation Research Center. This report does not constitute a standard, specification, or regulation.

March 2009



## ABSTRACT

The use of composite materials for strengthening the ailing infrastructure has been steadily gaining acceptance and market share. One can state that this strengthening technique has become main stream in some applications such as in strengthening of concrete structures. The same cannot be said about steel structures since research on composite strengthening is relatively new. Several challenges face strengthening steel structures using composite materials such as the need for high modulus composites to improve the effectiveness of the strengthening system.

In this study, the research team explores a new approach for strengthening steel structures by introducing additional stiffness to buckling prone regions in thin-walled steel structures. The proposed technique relies on improving the *out-of-plane* stiffness of buckling prone members by bonding pultruded fiber reinforced polymers (FRP) sections as opposed to the commonly used strengthening approach that relies on *in-plane* FRP contribution. This report presents the results from an experimental investigation where axial tension and beam specimens were tested to explore the feasibility of the proposed technique. Based on the results, one can conclude that this strengthening technique has great potential for altering failure modes by delaying the undesirable instability (buckling) failure mode. Preliminary analyses were also conducted and are presented in the report. Recommendations for future research efforts are made to expand the knowledge base about this yet unexplored strengthening technique.



## **ACKNOWLEDGMENTS**

This research was funded by the Louisiana Transportation and Research Center (LTRC) through the Transportation Innovation for Research Exploration (TIRE) program. The principal investigator (PI) would like to thank LTRC for allowing him to explore this novel strengthening technique that, to his knowledge, has never been tested before. The PI would like to acknowledge Walid Alaywan, P.E., from LTRC for his support of this exploratory research. His understanding of the challenges that faced the PI to conduct the experimental program is greatly acknowledged. Without his support, this project would not have been completed. The help of David Robertson from the Department of Civil and Environmental Engineering at Louisiana State University (LSU) in preparing the test specimens is also greatly acknowledged. The donation of materials by Fyfe Co., LLC and support from Strongwell is also greatly appreciated.

Any opinions, findings, conclusions, or recommendations expressed in this material are those of the authors and do not necessarily reflect the views of the sponsoring agencies.



## IMPLEMENTATION STATEMENT

The research presented herein is exploratory in nature. It confirms a long-held hypothesis by the PI that externally-bonded pultruded FRP sections can be used to enhance the capacity of steel structures where local buckling is the controlling mode of failure. Results from this research showed the great potential of the proposed strengthening technique for shear strengthening of buckling-prone webs. The concept, which has been proven to be effective in shear, can also be extended to flexure strengthening in cases where buckling of a compression flange is the controlling mode of failure.

This research, however, is only a proof of concept. Building on the findings of this research will require conducting more experiments to address two issues. First, the limitations of the proposed technique will have to be identified, which can be done via parametric studies (e.g., FRP material characteristics, epoxy material characteristics, buckling categorization of unstrengthened steel structure, FRP configurations). Second, the reliability of the proposed technique will need to be assessed. The findings from a study that covers the aforementioned experimental investigations together with an intensive analytical study are a minimum requirement before formal design provisions can be calibrated in order for engineers to implement this technique in every day design.



## TABLE OF CONTENTS

ABSTRACT.....	iii
ACKNOWLEDGMENTS .....	v
IMPLEMENTATION STATEMENT .....	vii
TABLE OF CONTENTS.....	ix
LIST OF TABLES .....	xi
LIST OF FIGURES .....	xiii
INTRODUCTION .....	1
OBJECTIVE .....	5
SCOPE .....	7
LITERATURE REVIEW .....	9
Composite Strengthening of Steel Structures .....	9
Bonding of Composite Materials to Steel Structures.....	11
METHODOLOGY .....	15
Experimental Program .....	15
Specimen Preparation and Material Properties.....	15
Instrumentation .....	18
Axial Tension Test.....	18
Beam Test .....	19
Finite Element Analysis.....	24
DISCUSSION OF RESULTS.....	29
Axial Tension Test.....	29
Beam Test .....	31
Preliminary Analysis Results.....	37
Eigen Buckling Analysis.....	37
Nonlinear Analysis.....	39
CONCLUSIONS.....	43
RECOMMENDATIONS.....	45
ACRONYMS, ABBREVIATIONS, & SYMBOLS.....	47
REFERENCES .....	49
APPENDIX.....	53
Design Calculations – Unstrengthened Beam Specimen.....	55
Material Properties.....	55
Geometry.....	55
Plate Girder Design.....	56
Tension Field Check .....	56
Compression Field Check (Lateral Torsional Buckling).....	56
Bearing Stiffener Design.....	60
Web Weld Design.....	62



## LIST OF TABLES

Table 1 Mechanical properties of GFRP pultruded section.....	16
Table 2 Mechanical properties of epoxy.....	16
Table 3 Summary of the tested specimens.....	24
Table 4 Ductility estimates for beam specimen.....	36
Table 5 Mode frequencies for beam specimen (Applied Load, $P = 100k$ ).....	39



## LIST OF FIGURES

Figure 1 Stiffening of thin-walled steel box girders .....	2
Figure 2 Proposed FRP stiffeners vs. conventional steel stiffeners.....	3
Figure 3 Comparison between different utilization modes of composite materials for strengthening.....	5
Figure 4 Stress-strain curve of the specimen material .....	16
Figure 5 GFRP material used in this study and steel surface preparation .....	17
Figure 6 Dimensions (not to scale) and test setup for axial tension specimen .....	19
Figure 7 Dimensions of beam shear specimen (unstrengthened) .....	20
Figure 8 Dimensions of beam shear specimen (strengthened) .....	20
Figure 9 Test setup for beam shear specimen (unstrengthened).....	21
Figure 10 Finite element analysis of first buckling mode.....	22
Figure 11 Straining actions in beam specimen due to applied loads .....	23
Figure 12 Finite element models of the steel girder .....	26
Figure 13 Boundary conditions and loads applied on FE models .....	27
Figure 14 Scalar parameters for geometric dimensions and number of element divisions used in ANSYS code .....	27
Figure 15 Performance of GFRP strengthened axial tension specimen .....	30
Figure 16 Progression of loading for beam specimens.....	32
Figure 17 Failure of beam specimens.....	34
Figure 18 Comparison between the behavior of stiffened and unstiffened beam specimens.	36
Figure 19 Deformed shape for first mode.....	37
Figure 20 Deformed shape for second mode .....	38
Figure 21 Deformed shape for third mode.....	38
Figure 22 Sensitivity of load-displacement curve to post-yield modulus (Model I – without FRP).....	40
Figure 23 Sensitivity of load-displacement curve to yield stress of steel (Model I – without FRP).....	41
Figure 24 Stress contours (S1) for models (a) without and (b) with the FRP stiffener just before failure .....	41



## INTRODUCTION

The prohibitive cost of replacing the aging civil infrastructure imposes a huge burden on owners and engineers to develop innovative, economical, and feasible strengthening techniques. Standard techniques for strengthening steel structures include welding, bolting or adhesive bonding of steel cover plates to the existing systems. The aforementioned techniques are feasible and have been extensively used in the field. However, they are susceptible to the following disadvantages:

- (1) sensitivity of the repaired system to fatigue problems due to stress concentrations produced by welding or bolting techniques,
- (2) dependence of the repaired system on the quality of field welding which is sometimes in question,
- (3) handling heavy steel plates complicates the installation,
- (4) long periods of service interruption during installation and need for cumbersome frameworks, and
- (5) vulnerability to corrosion is always present, especially in harsh environments.

In recent years, the use of composite materials in civil infrastructure applications started gaining acceptance. Structural strengthening is considered one of the most successful applications of composite materials in construction. This success is due in part to the superior properties that composite materials such as Fiber Reinforced Polymers (FRP) have to offer (e.g., high strength-to-weight ratio and environmental durability). Most of the successful applications reported in the literature are for strengthening structural elements made of concrete, masonry and wood. A quick review of the literature reveals that the majority of the published work has focused on the use of FRP materials such as glass and carbon FRP to provide additional capacity to tensile regions of deficient members. The additional tensile resistance adds to a beam's flexural capacity when the FRP is externally bonded to the tension side of a cross section subjected to bending moments [1]. Shear capacity also benefits from the additional tensile resistance provided by FRP when positioned to resist the diagonal tension caused by shear forces [2]. The success of these strengthening techniques and the wealth of information published in the literature about it have reached a mature stage such that guidelines and codes (e.g., [3], [4], [5], and [6]) have been drafted to assist engineers in the design and application of such systems.

A quick comparison between the application of composites for strengthening of steel and concrete structures shows that the former is relatively lagging in terms of the number of applications and available information. The lack of applications is due to the fact that steel

has superior mechanical properties (yield strength and elastic modulus) when compared to concrete; hence, the effectiveness of utilizing commonly used FRP's is greatly reduced since larger amounts would be needed. The availability of high modulus FRP materials in recent years shows potential for new steel strengthening applications [7]. As with all new materials, higher costs may be prohibitive and render this approach unfeasible from an owner's point of view.

The current study explores a different approach for structural strengthening in which the tensile capacity of the composite material is almost irrelevant. The strengthening is achieved by stiffening buckling prone regions using pultruded FRP sections, thus delaying premature unstable modes of failure and allowing for the strengthened material to achieve its full strength. The novel technique is particularly suited for thin-walled steel members where local buckling may be an issue. Thin-walled steel structures are always designed with stiffening components to prevent premature buckling failure modes. Figure 1 shows different stiffening elements inside a typical steel box girder bridge.

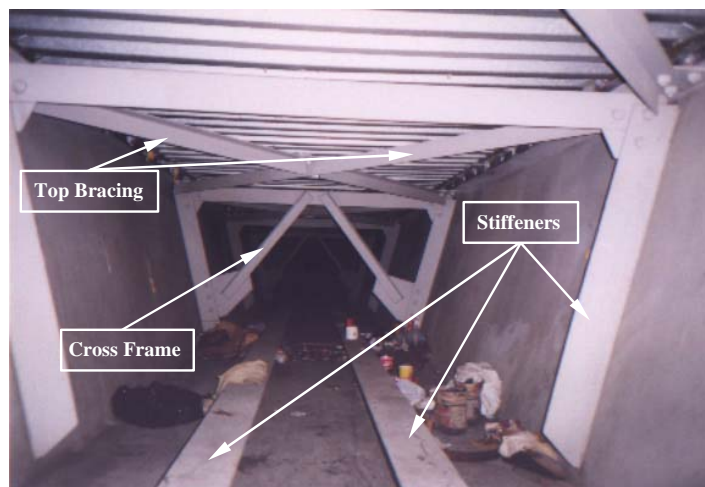
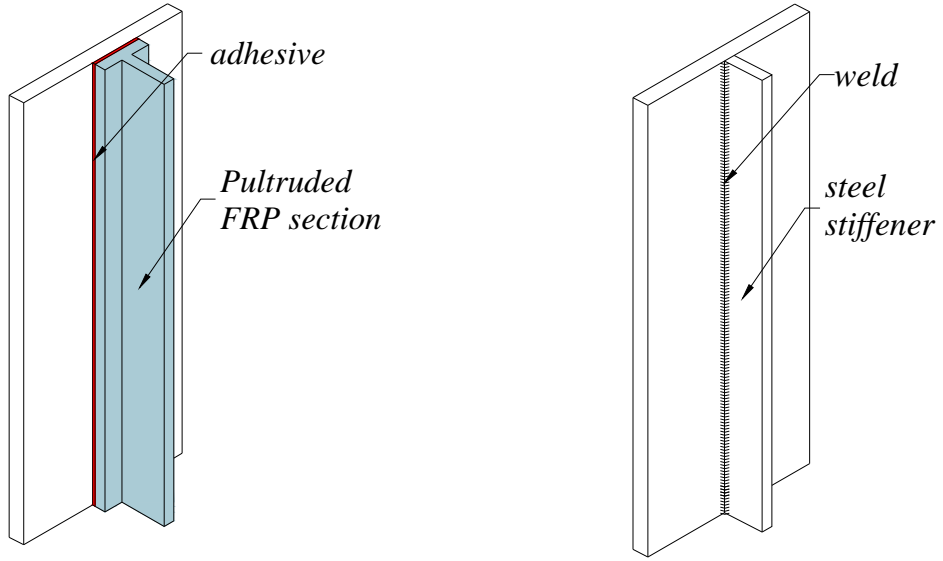


**Figure 1**  
**Stiffening of thin-walled steel box girders**

The proposed stiffening technique is illustrated in Figure 2, which shows a schematic of how a T-shaped pultruded FRP section may be used as a stiffener that serves the same function of a regular steel stiffener. A pilot experimental program is carried out to explore the effectiveness of the proposed technique. Details of the experimental program are described, and the results are presented. Finally, conclusions are drawn from the test results, and recommendations for future research efforts are made to expand the knowledge base about this unexplored strengthening technique.



**(a) Proposed epoxy-bonded FRP stiffener (b) Conventional welded steel stiffener**

**Figure 2**  
**Proposed FRP stiffeners vs. conventional steel stiffeners**



## OBJECTIVE

The objective of this study is to investigate the potential of a new strengthening technique whereby FRP pultruded sections are employed to stiffen buckling-prone thin-walled steel structures. The new proposed technique is completely different than other FRP strengthening techniques that have been reported in the literature. In the proposed technique, the out-of-plane stiffness of the pultruded section is the major contributing factor in the strengthening scheme. Classical FRP strengthening schemes rely on the in-plane strength (tensile capacity) of the composite material. The difference between the two techniques is illustrated in Figure 3. In Figure 3-a, three different in-plane strengthening schemes are shown for beams deficient in flexure, shear, and for columns deficient in axial load capacity. In all three cases, the tensile strength of the composite material is the main contributing factor to strength. In the case of flexure, additional tensile capacity is provided hence the flexural capacity of the member. Bridging shear cracks also adds tensile capacity to complement the resistance resulting from stirrups. Finally, confinement resulting from hoop stresses enhances the performance and capacity of concrete columns or piles. Conversely, the proposed technique, which is illustrated in Figure 3-b, relies on restraining the out-of-plane movement of the strengthened plate that may take place in buckling-prone regions. The in-plane strength of the FRP stiffener is almost irrelevant in the proposed strengthening technique. As demonstrated later, FRP stiffeners can be optimally oriented to contribute to the out-of-plane stiffness without sharing large portions of the in-plane load causing buckling in the strengthened plate.

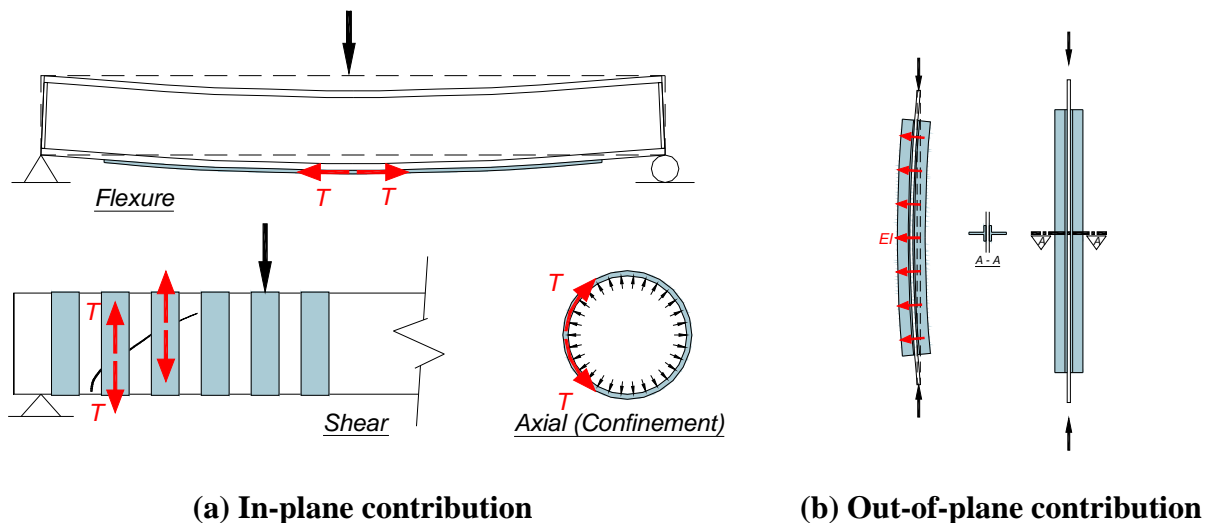


**Figure 3**  
**Comparison between different utilization modes of composite materials for strengthening**



## **SCOPE**

The proposed strengthening technique has the potential of enhancing the strength of thin-walled steel structures for a wide range of applications. Examples of such applications include web stiffening for improved shear strength and compression flange stiffening for improved flexural strength. The research conducted in this project is limited to shear strengthening where pultruded FRP sections were employed as stiffeners to a buckling critical web. Various types of pultruded FRP sections may be utilized for the same purpose. In this study, only glass FRP (GFRP) sections are used, which are among composites with low modulus of elasticity. Sections with higher modulus of elasticity were not covered in this study. However, because of their higher stiffness, their performance may be expected to at least match, if not exceed, that of GFRP stiffeners.



## LITERATURE REVIEW

The following is a summary of the work done by other researchers in fields related to this research.

### Composite Strengthening of Steel Structures

Standard techniques of steel structure strengthening include welding, bolting, or adhesive bonding of steel cover plates to the existing systems. The disadvantages of these techniques are corrosion effects, sensitivity of the repaired system to fatigue problems due to stress concentrations produced by welding or bolting techniques, long period of service interruption, and need of placing cumbersome frameworks. Recently, the use of epoxy-bonded FRP materials has become a promising alternative due to its high tensile strength, stiffness, and corrosion and fatigue resistance. However, failure of a FRP-strengthened steel member can occur due to: (1) top flange buckling in compression, (2) web buckling in shear, (3) FRP ruptures, and (4) debonding of FRP strips. Several studies have been conducted to assess the feasibility of strengthening steel members using FRP composites.

Recently, the use of epoxy-bonded FRP materials has become a promising alternative due to its high tensile strength, stiffness, and corrosion and fatigue resistance. Sen et al. tested six specimens consisting of  $W8 \times 24$  A36 steel acting compositely with a 102-mm thick by 711-mm wide reinforced concrete slab [8]. The composite girders were first loaded past yield of the tension flange. The damaged specimens were then strengthened using carbon fiber reinforced polymer (CFRP) laminates of different thicknesses (2 mm and 5 mm) bonded to the tension flange. For these systems CFRP/adhesive bonds were the weakest links and would control the failure mode. Hence, appropriate fasteners were used to increase the capacity of the adhesive. The authors concluded that (1) in order to achieve comparable strength and stiffness gain typically obtained in strengthened concrete and wood members, much thicker CFRP laminates are needed for strengthening steel composite members, (2) the estimated increase in ultimate strengths ranged from 11 percent to 50 percent depending on the yield strength of the specimen and mode of failure, (3) the failure mode was generally ductile and accompanied by considerable deformation, and (4) when epoxy adhesive was used alone for thicker (5 mm) laminates, adhesive failure led to the separation of CFRP laminates.

Vatovec et al. investigated the behavior of simple span, 11 ft. long,  $TS6 \times 6 \times 3/16$  grade A500 steel tubes strengthened with different CFRP configurations and loaded to failure [9]. 50 mm  $\times$  1.2 m Sika Carbodur<sup>TM</sup> S512 CFRP strips and SikaDur 30 epoxy adhesive were used in strengthening the steel tubes. To eliminate local buckling, some specimens had the

middle-half of their length filled with normal-weight concrete. Load was applied through a pair of point loads equidistant from the mid-span. The failure mode of steel tube specimens not filled with concrete was controlled by local buckling. An increase in strength was observed with the increase in number of CFRP strips for concrete filled tubes. For all the strengthened tubes with concrete infill, the failure mode was controlled by delamination of CFRP strip with top strips debonding prior to the bottom strips in all tested cases. The authors concluded that CFRP strips provide additional flexural capacity to the steel tubes, but the additional strength is limited by local failure modes and debonding of CFRP. The authors also concluded that if the load increase provided by the CFRP is limited, ductility of the composite member will not be compromised.

Tavakkolizadeh and Saadatmanesh also studied the behavior of steel-concrete composite girders strengthened using CFRP sheets under static loading [10]. Three composite girders, consisting of W355 × 13.6 A36 steel beams and 75-mm thick by 910-mm wide concrete slabs were strengthened using CFRP sheets of same thickness and different number of layers (1, 3, and 5) bonded at the tension flange. A two-component less-viscous epoxy was used for bonding the sheets to each other. The specimens were tested under four point bending. The authors concluded: (1) the ultimate load carrying capacity of the strengthened girders increased by 44, 51 and 76 percent for 1-, 3- and 5-layer CFRP sheets; (2) the efficiency for utilizing the CFRP sheet increased as the number of layers decreased, and at failure, stresses in the CFRP sheet reached 42 percent of its ultimate strength for the five-layer system while it reached 75 percent for the one layer system; and (3) the analytical models (Hogenstad's parabola and AASHTO's method) provided conservative results in predicting ultimate capacity of the strengthened girder.

Al-Saidy et al. presented the results of an experimental study of the behavior of CFRP strengthened steel-concrete composite girders [11]. Strengthening was achieved by attaching the CFRP plates to the bottom flange and, in some cases, to the beam web. Two types of CFRP plates with different tensile modulus of elasticity were used to investigate the effect of their stiffness. It was concluded that (1) up to 45 percent strengthening can be achieved through the use of CFRP plates; (2) at the failure load of the control beam, deflection of the strengthened beam was 25 percent of that of the control beam; and (3) ductility was slightly reduced with the addition of CFRP plates.

Fawzia et al. investigated the behavior of very high strength (VHS) circular steel tubes strengthened by CFRP and subjected to axial tension [12]. Multilayer high modulus MBrace CF530 (640 GPa) and high strength epoxies (Araldite 420) were used in the strengthening process. The strain distribution along the CFRP bond length and layer thickness was studied.

High modulus (HM) CFRP was found to be superior to normal modulus CFRP in retrofitting steel tubes. For steel tubes bonded with HM CFRP system, effective bond length was found to be around 50 mm. However, for normal modulus CFRP, the value is 75 mm. Across the CFRP layer, a decrease in strain distribution from bottom to top layer was observed.

Shaat and Fam studied the behavior of axially loaded short and long square hollow structural section (HSS) columns strengthened with CFRP sheets [13]. Different CFRP sheet orientations in the longitudinal and transverse directions were studied. A maximum strength gain of 18 percent was achieved for short columns with two transverse CFRP layers. For long columns, the maximum strength gain of 23 percent was achieved with three longitudinal CFRP layers applied on four sides. In all CFRP-strengthened long columns, lateral deflections were reduced. Strength gain in long columns was highly dependent on the column's imperfection. As such, no correlation was established between gain in strength and the number of CFRP layers. The strengthening of cast iron struts that support brick walls of a vent shaft in a London Underground line was reported by Moy and Lillistone [14]. The cruciform section was chosen by Victorian engineers because it provided good buckling resistance in both directions. Additional loads were imposed on the struts due to ground movement, which led to an investigation into appropriate strengthening schemes. The special nature of cast iron, which is brittle and relatively weak in tension, led to the consideration of FRP and a possible strengthening alternative. Results from six specimens tested in compression showed that the ultra high modulus (UHM) CFRP bonded well with the cast iron section and enhanced the performance of the strengthened struts. The final failure of the strengthened struts was initiated by CFRP fibers reaching their compressive capacity followed by failure of the cast iron on the tension side. Based on the findings of this research, a plan was devised to strengthen the deficient struts in the underground line.

### **Bonding of Composite Materials to Steel Structures**

The limitations of using CFRP reinforcements are the intolerance to the uneven bonding surface, potential brittle failure modes, and lack of durability of the adhesive joints. The weakest link in plate bonding of CFRP laminates to metallic adherent is the adhesive bond. Wide range of adhesives can be used to bond CFRP to metallic elements including epoxy, polyurethanes, acrylics, or cyanoacrylate. However, epoxy is the most commonly used adhesive for steel and CFRP bonding. Several researchers conducted studies to characterize and model the debonding failure of epoxy adhesives and to determine the adequate bonding technique.

Sen et al. carried out nonlinear finite element analyses to evaluate the adequacy of epoxy adhesive under extreme conditions [8]. The results indicated that high peeling stresses would

cause the failure of the epoxy at the end of the CFRP laminate. To prevent this type of failure, additional bolting was required. For the configurations that dictate shear transfer using bolts, the use of adhesive would still be recommended to help distribute the load and provide transfer of shear until the bolts become fully loaded in bearing. Larger quantities of smaller bolts should be used to reduce the tendency for transverse CFRP laminate fractures and to minimize the magnitude of localized stress concentrations at the bolts. However, for thinner laminates bonded using epoxy alone, smaller tensile forces were developed, and the associated shear stress never exceeded the epoxy's shear strength.

Miller et al. performed experimental and analytical studies to quantify force transfer between steel/CFRP adherents and epoxy adhesives [15]. The study is important since the length and position of termination of the plate determines the rate of force transfer and corresponding development length. High peeling stresses are another important issue that might cause failure of the epoxy at the end of the CFRP laminate. The authors also showed that to effectively limit the peeling stresses, CFRP plates should be beveled to  $45^\circ$  at all terminations.

Hollaway and Cadei reviewed various techniques to provide bonding between steel and advanced polymer composite (APC) [16]. They recommended using epoxies that are compatible with curing conditions. Although epoxies with most desirable properties require curing at elevated temperatures, epoxies that can be cured at ambient temperatures are most suitable for civil engineering applications. Surface preparation of steel and CFRP sheets is very important for the durability of the adhesive bonding. Metallic surfaces to be bonded must be: (1) free from contamination which can be achieved by degreasing; (2) chemically active (typically obtained by surface abrasion or etching) to enable the formation of chemical bonds between adhesive and adherent; and (3) resistant to environmental deterioration in service especially due to hydration. Hydration can be resisted through chemical modification of the surface. The composite material (CFRP) usually contains peep-ply, a sacrificial layer of glass fiber and polymer material, on one or both surfaces and would be removed immediately before applying the epoxy adhesive to it. Although CFRP is usually corrosion resistant, since carbon fibers are electron conductors, galvanic interaction can take place when it comes in contact with metals. Presence of electrolytes such as sea water may boost up the process. Hence, to prevent the galvanic action, a corrosion barrier (glass fiber layer) should be placed between two adherents during the bonding process.

Buyukozturk reviewed the research progresses achieved in understanding debonding problems in reinforced concrete and steel members strengthened using CFRP composites [17]. Previous studies showed that debonding takes place in high stress regions and is often associated with material discontinuities or presence of cracks. Improper selection of adhesives might promote this type of failure. Buyukozturk also found that for a fixed CFRP ratio, the potential for debonding increases with the increase in CFRP thickness.

In another study by Colombi and Poggi, the effectiveness of using adhesively bonded CFRP laminates to strengthen tensile steel members and bolted joints was investigated experimentally and analytically [18]. Common applications of CFRP plates such as double side reinforcement of continuous steel plates, double lap joints, and bolted joints were considered. All the experiments were subjected to axial tensile load. Two different types of epoxy adhesives (Sikadur 30 and Sikadur 330) were used to bond the CFRP laminates to the steel structures in a double lap joint. The reinforcements and the joints realized by Sikadur 30 exhibited a ductile behavior since the debonding of the reinforcements was observed only after the yielding of the steel plates. Failure mode was interfacial failure at the steel-adhesive interface. The application of Sikadur 330, on the other hand, produced brittle behavior of the specimen and the recorded failure mode was an inter-laminar composite strip delamination. Two experiments on steel bolted joints reinforced with CFRP plates were conducted, and reasonable increment in the failure load was achieved in one case. Sebastian and Luke studied the stress-transfer mechanics in the interface between steel plates and strengthening elastic strips [19]. Seven beam specimens were tested with different CFRP configurations including one specimen (B5) where the strengthening CFRP strips were bonded to the compression side. A 300 mm region at midspan was left unbonded between the compression flange CFRP strengthening strip to simulate an adhesive defect in Specimen B5. The failure of this specimen was controlled by CFRP strip buckling which buckling propagated along the top of the specimen starting at the unbonded region at midspan. The results showed that the steel compression flange transmitted the loads directly to the CFRP strips.

An excellent compilation of knowledge and efforts by various researchers were compiled by Schnerch et al. [20]. Based on the best practices reported in the literature, the authors proposed guidelines and installation techniques for the strengthening of steel bridges with CFRP materials. The guidelines include the design criteria for flexural strengthening of typical steel-concrete composite girders using HM-CFRP material whose elastic modulus is three times that of the steel. The authors concluded that HM CFRP material provide a promising alternative for strengthening steel bridges. The proposed design procedure accurately predicted the behavior of a steel-concrete composite beam strengthened with HM CFRP materials.

One can see from the review of published work that FRP strengthening of steel structures has mainly focused on in-plane contributions of composite plates, strips, and sheets. In most cases, CFRP was the material of choice to improve the effectiveness of the strengthening system. This study explores a different approach whereby low-modulus GFRP pultruded sections are used to improve the out-of-plane stiffness of buckling prone steel members.

## METHODOLOGY

Because of the novel nature of this research, the PI's literature search did not reveal any established methodologies for the proposed strengthening technique. It was therefore concluded that the general methodology followed in most new research efforts also be followed in this study. Results from a study that relies solely on analytical investigations would always be viewed with skepticism until its findings are validated experimentally. It was therefore deemed necessary that an experimental program be conducted followed by laying out the framework of analytical studies of the problem.

The purpose of the experimental program was two-fold. First, it was used to validate the concept of using low-modulus FRP pultruded sections to stiffen thin-walled steel structures. It was also used to compare the proposed novel technique to the classical approach of FRP strengthening where the in-plane contribution of the composite material is always relied on.

Details of the experimental program are provided next.

### Experimental Program

A pilot experimental program was devised to validate the feasibility of the proposed strengthening technique. Two types of specimens were tested, namely axial tension and beam shear specimens. The purpose of the axial tension specimen is to provide a benefit comparison between the commonly used approach and the new proposed technique. The former relies on in-plane FRP contribution to the behavior of the strengthened member, while the latter enhances its strength by relying on the out-of-plane stiffness of the geometric properties of pultruded FRP sections.

### Specimen Preparation and Material Properties

The steel used in this study was A36 steel. The stress strain relationship obtained from standard coupons can be seen in Figure 4 [21]. The motivation behind this study was to demonstrate the feasibility of using low modulus FRP in strengthening steel structures. Glass FRP (GFRP) pultruded sections were chosen for the study. Wide-flange beams manufactured by Strongwell were chosen for the study. The EXTREN<sup>®</sup> Series 500 6 in. x 3/8 in. sections were used throughout this study. Table 1 lists the basic material properties of the GFRP sections. It should be noted that the modulus of elasticity of this material is 2,500 ksi, which is substantially lower than that of steel. Nevertheless, it will be demonstrated that the proposed strengthening technique can still be effective even with low modulus FRP materials. A two component epoxy was used to bond the GFRP sections to the steel specimens. The epoxy (Tyfo S<sup>®</sup>) is manufactured by Fyfe Co. and is intended for use with

fiber wrap systems. While other superior epoxies may be better suited for steel applications, this epoxy was chosen for the study to demonstrate that regular epoxies can still be used for applying the proposed strengthening technique. Table 2 lists the mechanical properties of the used epoxy.

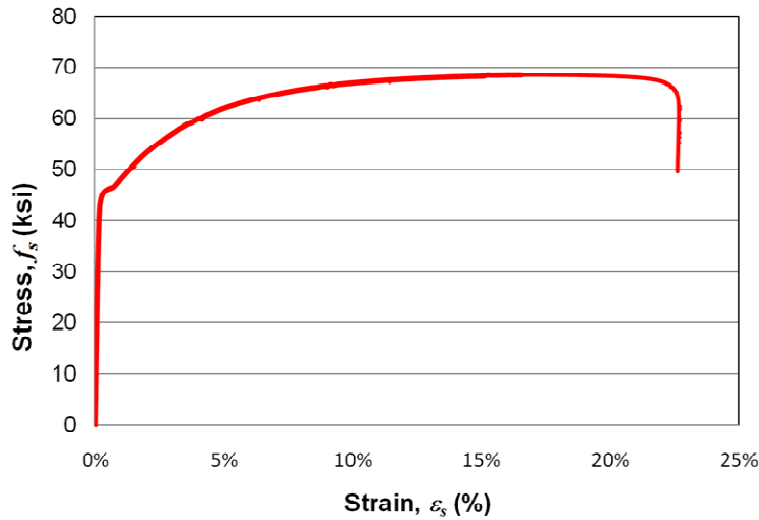


**Figure 4**  
**Stress-strain curve of the specimen material**

**Table 1**  
**Mechanical properties of GFRP pultruded section\***

Property	Value
Tensile Stress, MPa [ksi]	138 [20]
Flexural Stress MPa [ksi]	207 [30]
Modulus of Elasticity MPa [ksi]	17,200 [2,500]

\* As provided by the manufacturer [22]

**Table 2**  
**Mechanical properties of epoxy\***

Property	Value
Tensile Stress, MPa [ksi]	50 [7.25]
Tensile Modulus, MPa [ksi]	3,180 [461]
Flexural Stress MPa [ksi]	123 [17.90]
Flexural Modulus MPa [ksi]	3,120 [452]
Elongation [%]	5.0

\* As provided by the manufacturer [23]

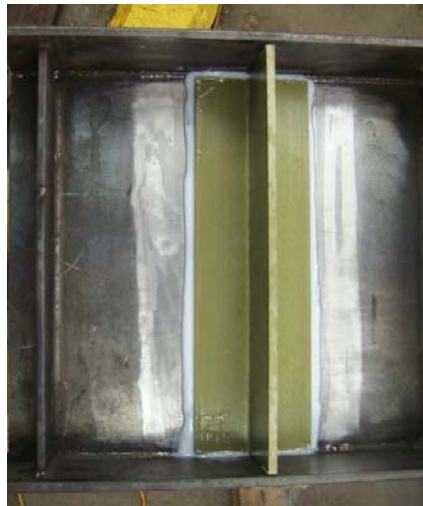
The GFRP stiffeners were cut from a pultruded wide-flange beam section using a table saw equipped with a concrete cutting blade. The beam section was first cut to the desired length, and then the flange was cut on one side to obtain a T-shaped section that will serve as the GFRP stiffener. The plate resulting from the separated flange was further cut to make rectangular sections for the axial tension specimens. Figure 5-a and b show the original WF-beam and the final T-shaped stiffener, respectively. Before bonding the GFRP sections to the steel surface, all rust was removed using coarse sandpaper followed by a steel brush. The goal was to reveal the *white* metal for enhanced bonding as can be seen in Figure 5-c [20]. On the GFRP side, the final glazed surface of the pultruded section was also removed and irregular scratches were made to enhance bonding as well. Both bond surfaces were cleaned with acetone to remove any residual particles that may adversely affect bonding. No pressure was applied on the GFRP sections other than what is needed to squeeze excessive epoxy from in between the two surfaces. Figure 5-c shows the pultruded T-shaped stiffener after installation on the web of the steel beam. The epoxy was applied to both surfaces, and then the GFRP stiffener was positioned in the desired location.



**(a) Original wide-flanged GFRP section**



**(b) Final T-shaped stiffener**



**(c) Steel surface preparation for epoxy bonding.**

**Figure 5**  
**GFRP material used in this study and steel surface preparation**

## **Instrumentation**

During the test, the following quantities were recorded: (1) applied load, (2) deformation under the load, and (3) strain at the top fiber of the bottom flange (beam shear specimen) and at mid-height (axial tension specimen). This data was continuously recorded at small time increments, which were also recorded. The second beam test was further instrumented on the web with strain gages and fiber optic sensors. The purpose of the web instrumentation was to study the ability of fiber optic sensors to detect buckling, which is beyond the scope of the research. Nevertheless, it provided valuable information regarding the stress state in the web.

## **Axial Tension Test**

The axial tension specimen used in this study was obtained from a quarter of an in. thick ASTM A36 steel plate cut by a hydrocut waterjet machine. The dimensions of the dog bone specimen grips and cross section followed the rectangular plate-type standard dimensions addressed in ASTM Standard E8 [21]. The specimen's length was chosen to be 30 in., which is longer than the 18 in. called for by the ASTM standard. This modification was made to allow for tangible FRP contribution to the longitudinal stiffness, which may be affected by the FRP development length. Figure 6-a shows the dimensions of the steel plate specimens. Two 0.95 in. x 0.375 in. x 19.5 in.-GFRP plates were bonded to both sides of the specimen as can be seen in Figure 6-b. The test was conducted using MTS 810 Materials Testing System (Capacity 55 kips) equipped with MTS Hydraulic grips and controlled by an MTS TestStar II controller.

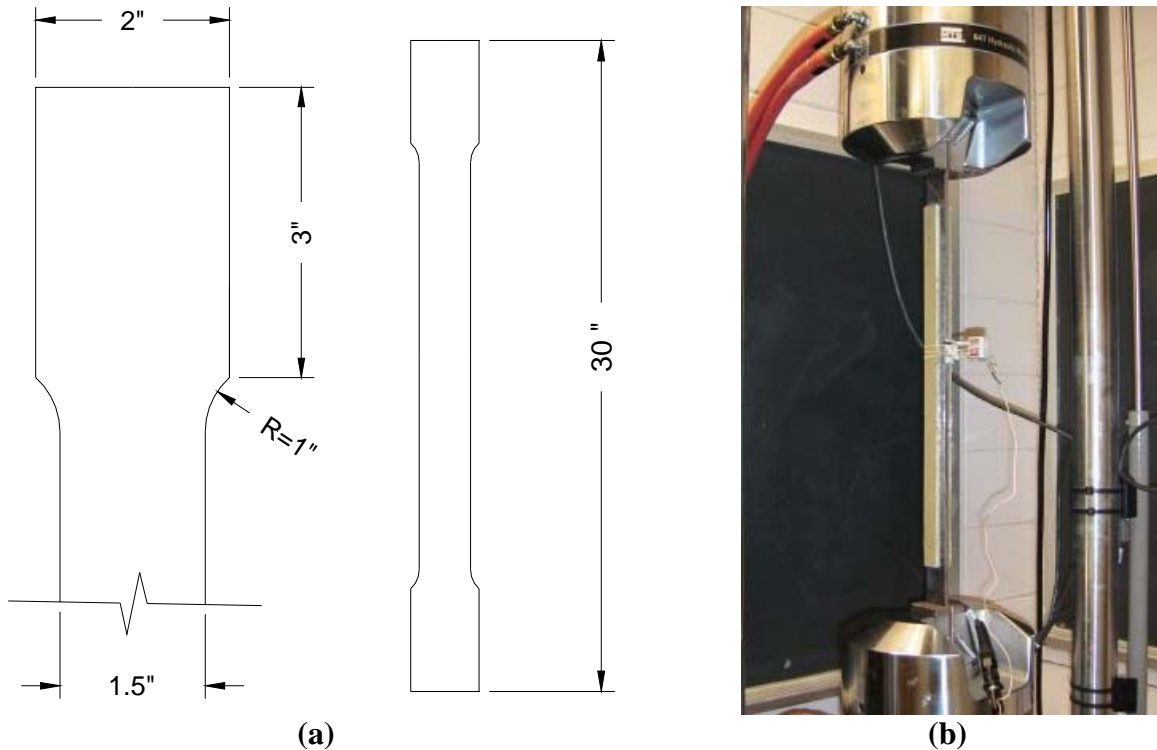


**Figure 6**  
**Dimensions (not to scale) and test setup for axial tension specimen**

### Beam Test

The beam specimens used in this study were designed to achieve the stated objective of investigating the feasibility of utilizing low modulus FRP sections as stiffening components for buckling prone regions in thin-walled steel structures. Web buckling was chosen as the intended mode of failure of the steel beam, which was achieved by overdesigning all other possible modes of failure (flexure, local flange buckling, steel stiffener buckling, welding and load bearing) for the unstrengthened section by a factor of at least 2.0. The Appendix provides details about the design calculations for the unstiffened specimen. Figure 7 shows the dimensions of the built-up steel beam specimens used in this study. One GFRP stiffener was bonded to each side of the steel web in a vertical orientation as can be seen in Figure 8. The choice of a vertical orientation was deliberately chosen over a diagonal compression strut orientation (i.e., connecting the top flange under the load to the bottom flange at the support) to avoid applying a large compression force on the stiffener that may cause a premature failure of the stiffener. This choice was made based on a buckling analysis that was carried out before testing using the general purpose finite element (FE) analysis package ANSYS [24]. The loading setup for beam tests can be seen in Figure 9. Figure 10 shows the FE mesh of the beam specimen used in this study (described in details later), the first buckling mode without GFRP stiffener, and the out-of-plane deformation of the end panel's

web. One can see in Figure 10-c that the vertical orientation of the GFRP stiffener covers, i.e., stiffens, a large portion of the web that would deform out of plane under high shear loads. More details about the analysis are discussed later in this report.

A single point load was applied over the first internal stiffener. As can be seen Figure 11 from the Shear Force Diagram of the loaded beam specimen, this loading subjected the first panel to three times the shear force acting on the rest of the beam. The strengthened specimen was provided with a GFRP stiffener to assist the first panel in resisting its tendency to buckle out of plane because of the high shear forces.

Table 3 lists the specimens tested in this study.

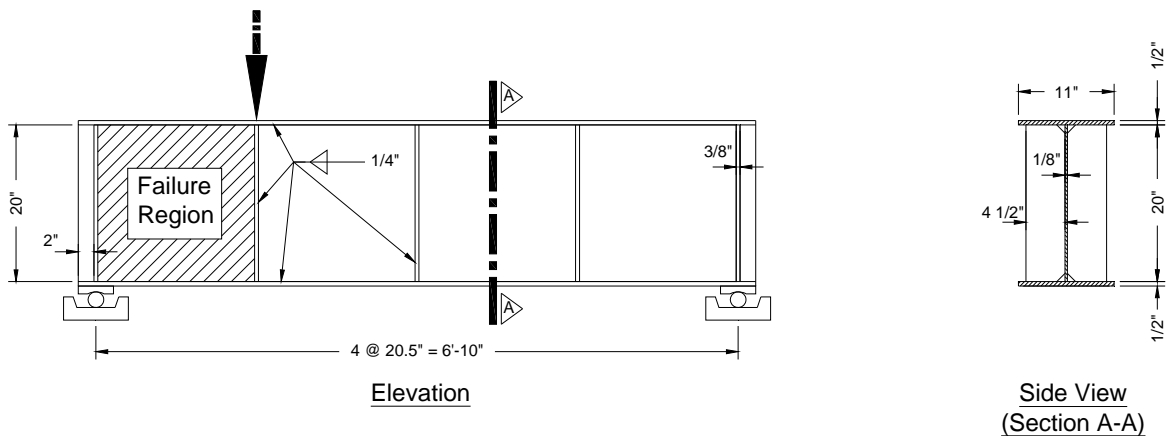


**Figure 7**  
**Dimensions of beam shear specimen (unstrengthened)**

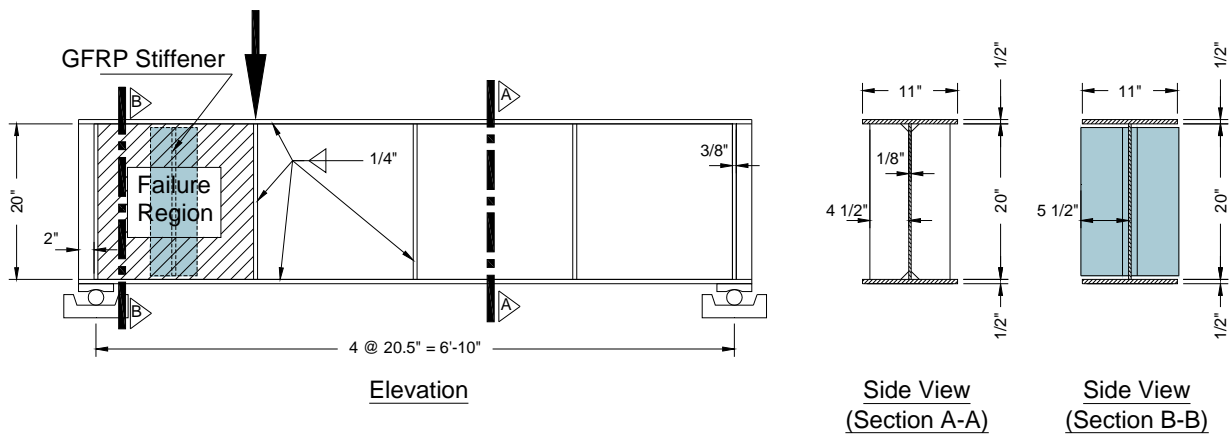
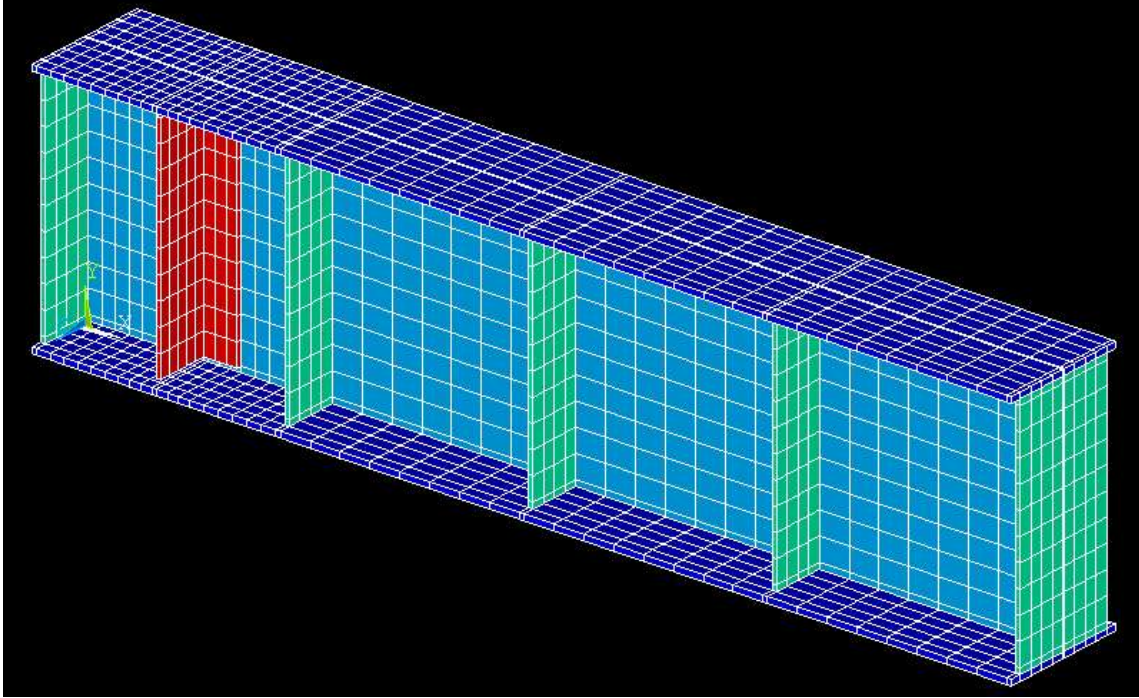


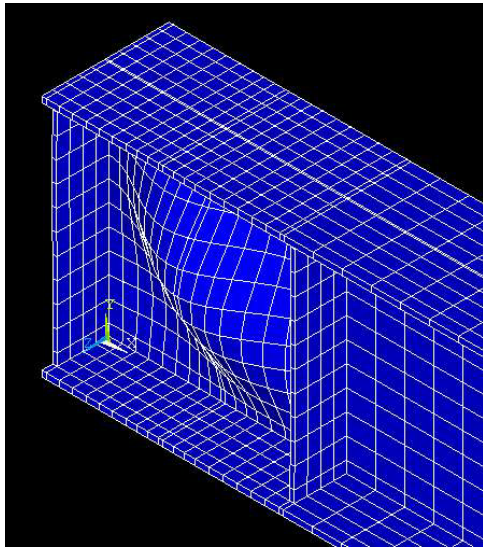
**Figure 8**  
**Dimensions of beam shear specimen (strengthened)**



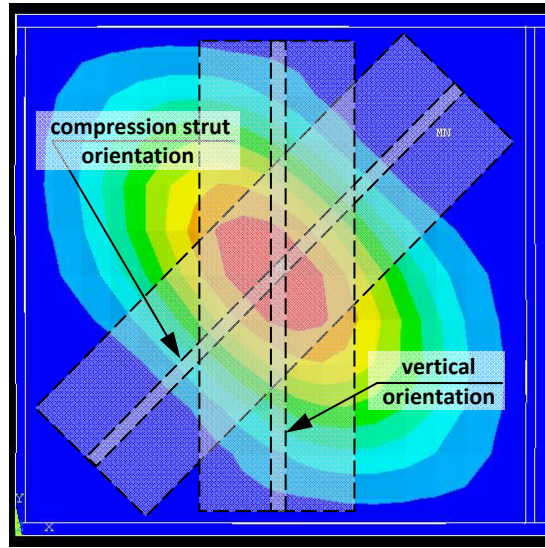
**Figure 9**  
**Test setup for beam shear specimen (unstrengthened)**



(a) Finite element mesh used in eigenvalue analysis



(b) First buckling mode



(c) Contours of out-of-plane deformation (end panel)

**Figure 10**  
Finite element analysis of first buckling mode

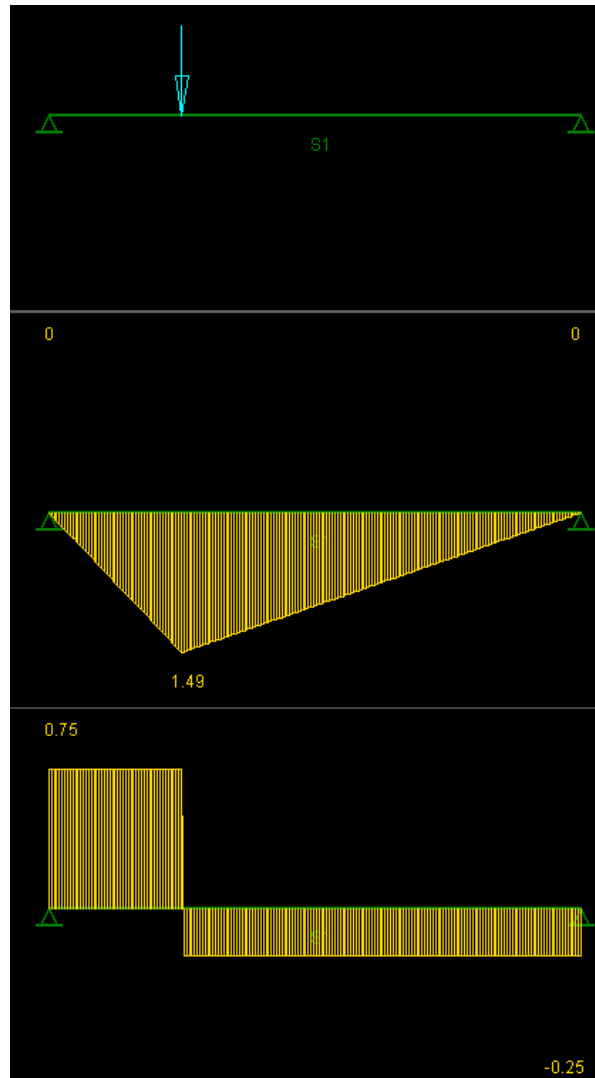


**Figure 11**  
**Straining actions in beam specimen due to applied loads**

**Table 3**  
**Summary of the tested specimens**

Test #		Stiffening	Test Mode	Notes
Axial Specimens	A1	–	Tension	Standard sheet coupon [21]
	A2	1 plate / side		Modified plate coupon [21]
Beam Specimens	B1	–	Shear	Built-up beam
	B2	1 T-shape / side		Built-up beam

### Finite Element Analysis

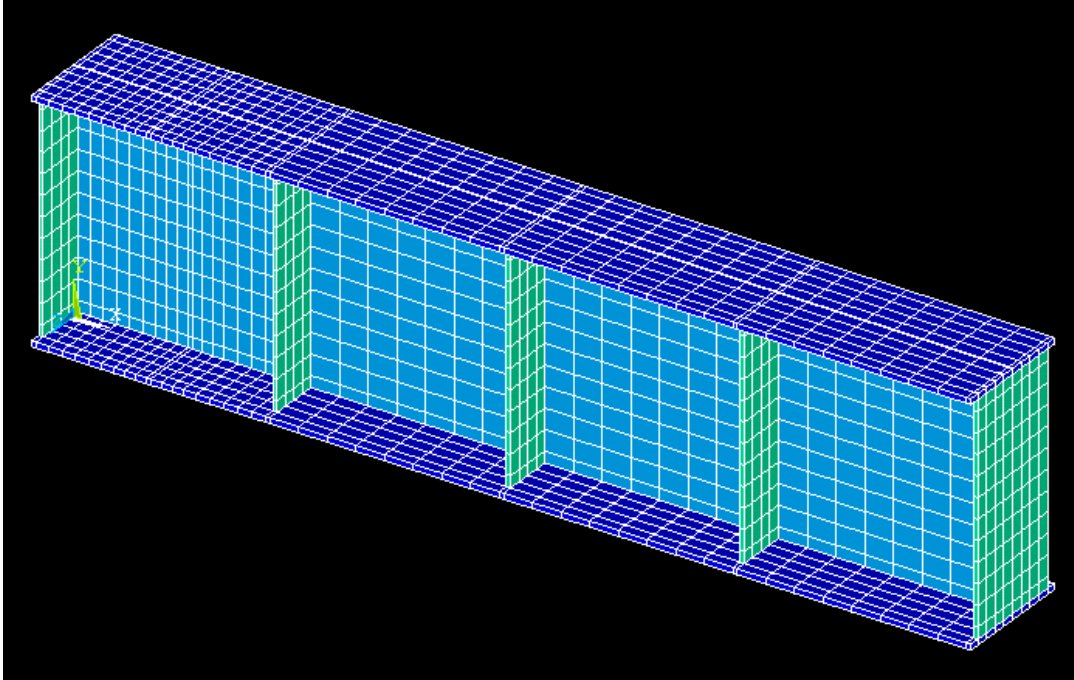
Two Finite Element (FE) models were created for the beam specimens. The purpose of the FE models is to establish the appropriate methodology for analyzing this type of strengthening technique. The FE models can then be used to assess the feasibility of FRP pultruded sections in stiffening steel girders by conducting parametric studies after they are validated using the experimental results obtained in the lab. The ANSYS general purpose FE package was used for the task as it provides superior nonlinear geometric and material capabilities that are essential for this study [24]. Figure 12-a and b show typical models of the steel girder without (Model I) and with (Model II) the FRP stiffeners, respectively. In Model II, the T-shaped FRP stiffeners were added to both sides of the first panel to simulate the physical configuration used in the lab. The SOLID 65 element type from the ANSYS element library was used to model both the steel girder and FRP stiffener. SOLID 65 element has a three-dimensional modeling capability of solids. It can model concrete components with or without reinforcing bars (rebars) and is capable of cracking in tension and crushing in compression including cracking in three orthogonal directions, crushing, plastic deformation, and creep. Furthermore, nonlinear material properties can be assigned to this element. Figure 13 shows the boundary conditions and applied load used in the FE model. The applied load was distributed over two lines of nodes above the first interior stiffener. This arrangement simulates the way the load was applied in the lab as the loading tip was in contact with the entire width of the top flange. In preparation for the parametric study that will be needed in the future, a dynamically variant model code was created where geometric dimensions are entered as variables that can easily be change without having to manually remesh the entire structure. Figure 14 shows the geometric parameters and number of element divisions used in generating the model.

The two types of FE analyses conducted in this study were:

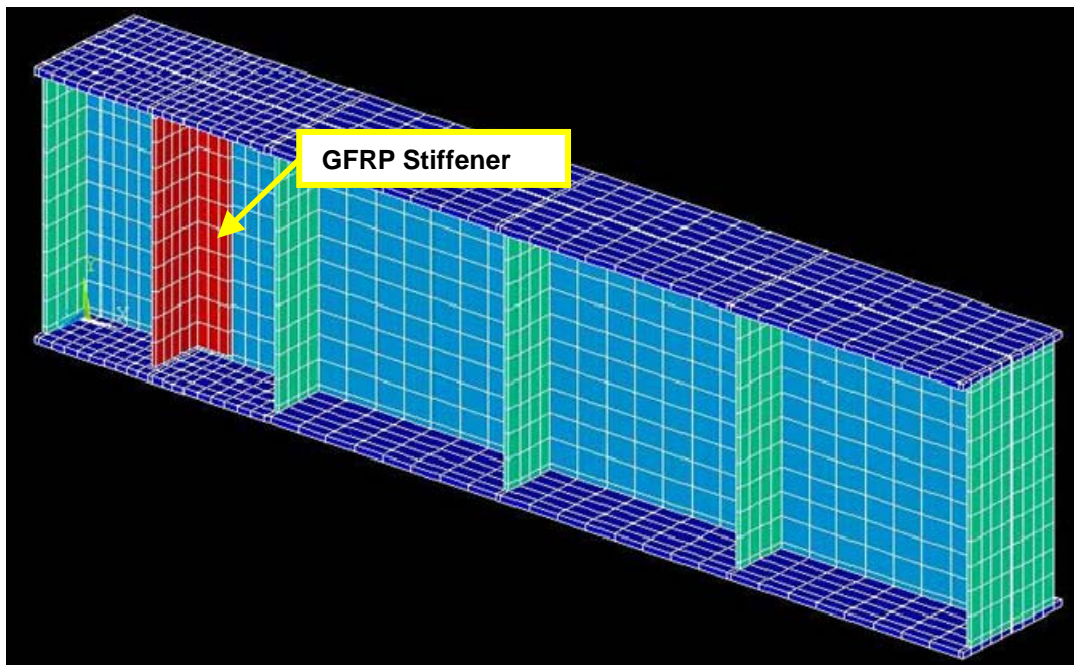
1. Eigenvalue analysis
2. Nonlinear plastic analysis

Each of the two analysis types offers valuable information for this type of problem. The eigenvalue analysis is often used in structural analysis to decompose complex behaviors in unique uncoupled behaviors. This is done via transformations similar to those used in dynamic analysis of structural members. The mode shape corresponding to each natural frequency can be uniquely identified using an eigenvalue analysis. Similarly, the unique buckling modes of a complex structure can be identified using the same approach. The eigenvalues correspond to the loads that are needed to initiate the buckling for each of the modes. Buckling analysis using the eigenvalue method is linear elastic; nevertheless, it provides valuable information as will be seen later.

The nonlinear plastic analysis is a monotonic static analysis where material and geometric nonlinearities are accounted for. By gradually loading the model in a manner similar to the conducted experiment in the lab, the model should exhibit the same behavior as that observed experimentally. However, numerical models are ideal geometries with perfectly aligned dimensions. Therefore, initiation of buckling is not possible in many cases. This is similar to the case of applying compression to a slender column. If buckling is not initiated, the column would *theoretically* fail by plasticization of the material. In real life, imperfections such as preliminary distortions facilitate the initiation of buckling. In this study, initial imperfections were introduced to the model by modifying the *ideal* geometry using the results from the eigenvalue analysis. The first mode is used for that purpose by imposing a fraction of its value as an initial imperfection on the model.



(a) Model I (without FRP stiffener)



(b) Model II (with FRP stiffener)

Figure 12  
Finite element models of the steel girder

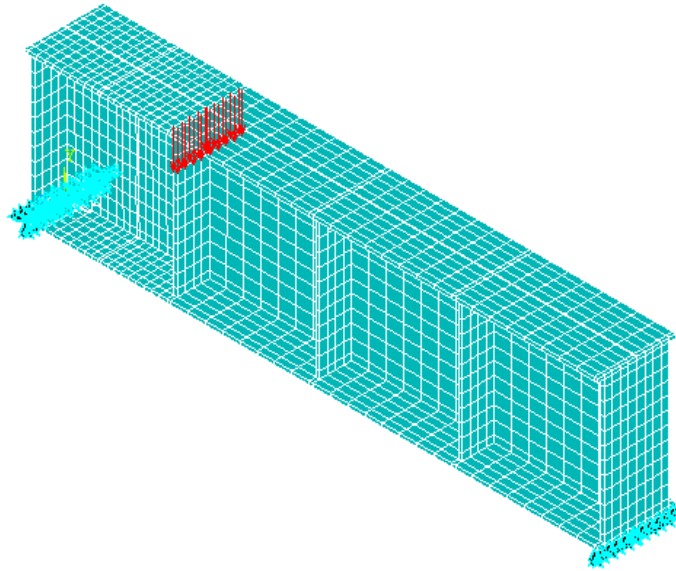


**Figure 13**  
**Boundary conditions and loads applied on FE models**

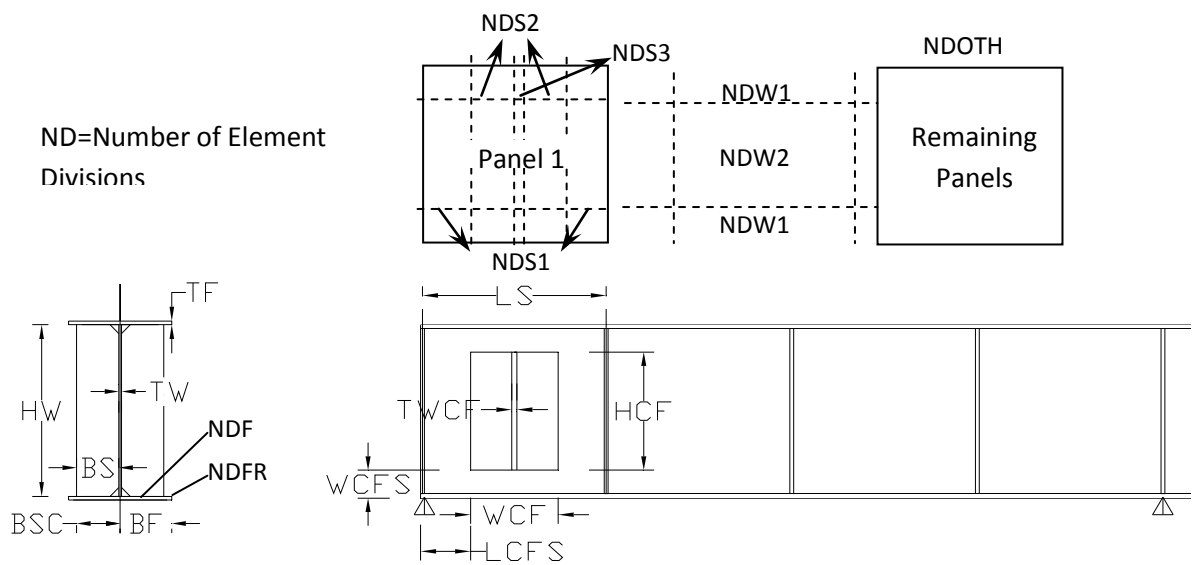


**Figure 14**  
**Scalar parameters for geometric dimensions and number of element divisions used in ANSYS code**



## DISCUSSION OF RESULTS

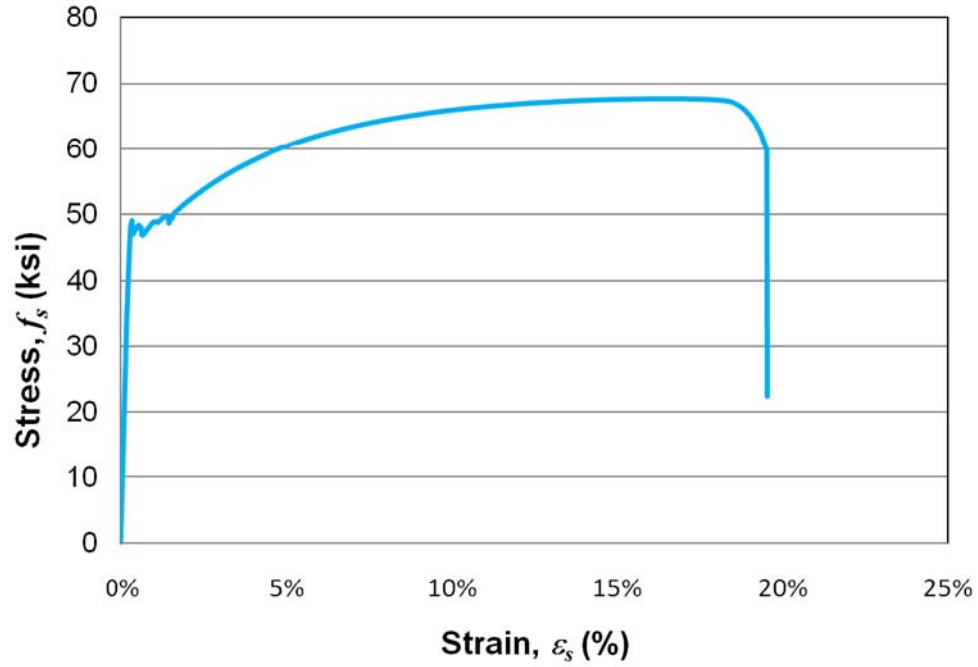
### Axial Tension Test

The axial tension specimen failed by debonding of the GFRP plates at a pre-yield strain level, which was then followed by typical yield and post-yield behavior up to rupture. This is evident from the plots shown in Figure 15. The stress strain relationship in Figure 15-a of the strengthened GFRP specimen is almost identical to that obtained from the bare steel coupons (see Figure 4). Therefore, assessment of the performance of stiffened specimen will be conducted using the axial stiffness,  $K_{\text{axial}}$ , which is defined as

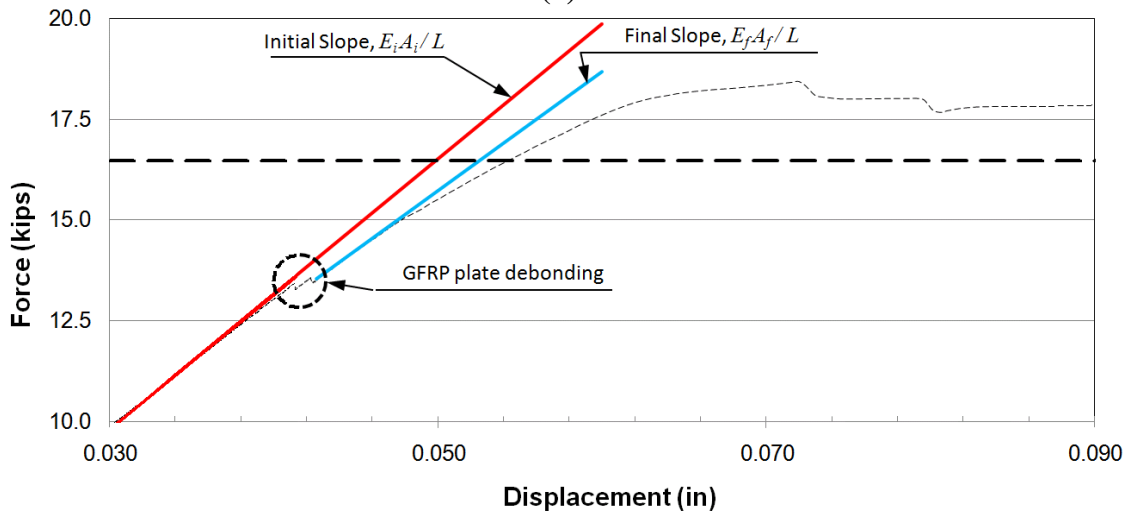
$$K_{\text{axial}} = \sum \frac{EA}{L} \quad (1)$$

where,  $E$  is the modulus of elasticity,  $A$  is the cross sectional area, and  $L$  is the specimen's length.

Figure 15-b is a plot of the force-displacement levels at which debonding occurred. This plot reveals that the *initial* axial stiffness of the GFRP-strengthened specimen,  $E_i A_i / L$ , was enhanced by about 13 percent prior to debonding as compared to the bare steel specimen. Once debonding takes place, the *final* axial stiffness of the specimen,  $E_f A_f / L$ , falls back to the original bare steel values. Hand calculations of the theoretical improvement of axial stiffness show that an increase of about 17 percent should be expected. The difference between the theoretical value and the experimentally measured one could be due to the fact that the GFRP is not fully effective in its contribution to the steel specimen's stiffness. Reasons for the partial effectiveness could be due to the development length after which the FRP is fully contributing to the system. A 25.4 mm (1 in.) of development length at each end of the GFRP plates constitutes about 10 percent of the total GFRP contribution. Finally, it can be said that while the strength of the stiffened steel section was not enhanced, it still gained axial stiffness. Thus, it can be stated that by bonding FRP plates to steel members of an excessively flexible structure such as a moveable bridge, deformations may be reduced due to the increase in stiffness.



(a)



(b)

**Figure 15**  
**Performance of GFRP strengthened axial tension specimen**

## Beam Test

The GFRP-stiffened beams performed substantially better than the axial tension specimens. The first specimen (unstiffened case) failed by buckling of the web as predicted by design. The failure load was 62.5 kips which was on a horizontal plateau following the initiation of buckling. The first visible web buckling was observed at a load equal to 56.0 kips. Figure 16 shows both tested beams at different loading stages during the tests. The figure is a visual documentation of the beams' behavior under equal loads starting at elastic loads and up to failure. Figure 17-a shows the beam conditions right after the initiation of buckling ( $P = 56.0$  kips) and at test end ( $P = 62.5$  kips). A substantially enhanced performance was demonstrated by the GFRP stiffened specimen. Failure occurred at a load equal to 87.5 kips. That is an improvement of 40 percent over the maximum load of the unstiffened specimen ( $P = 62.5$  kips), and an improvement of 56 percent if the load at the initiation of buckling ( $P = 56$  kips) is used as a reference point. Figure 17-b shows that the specimen was intact until the beam failed by debonding of the GFRP stiffener followed by immediate buckling of the web. Prior to this final load step, cracking noises were heard indicating the initiation of debonding. However, most of the epoxy cracks were not visible as they were under the GFRP stiffener with only a few cracks that could be seen at the edges.

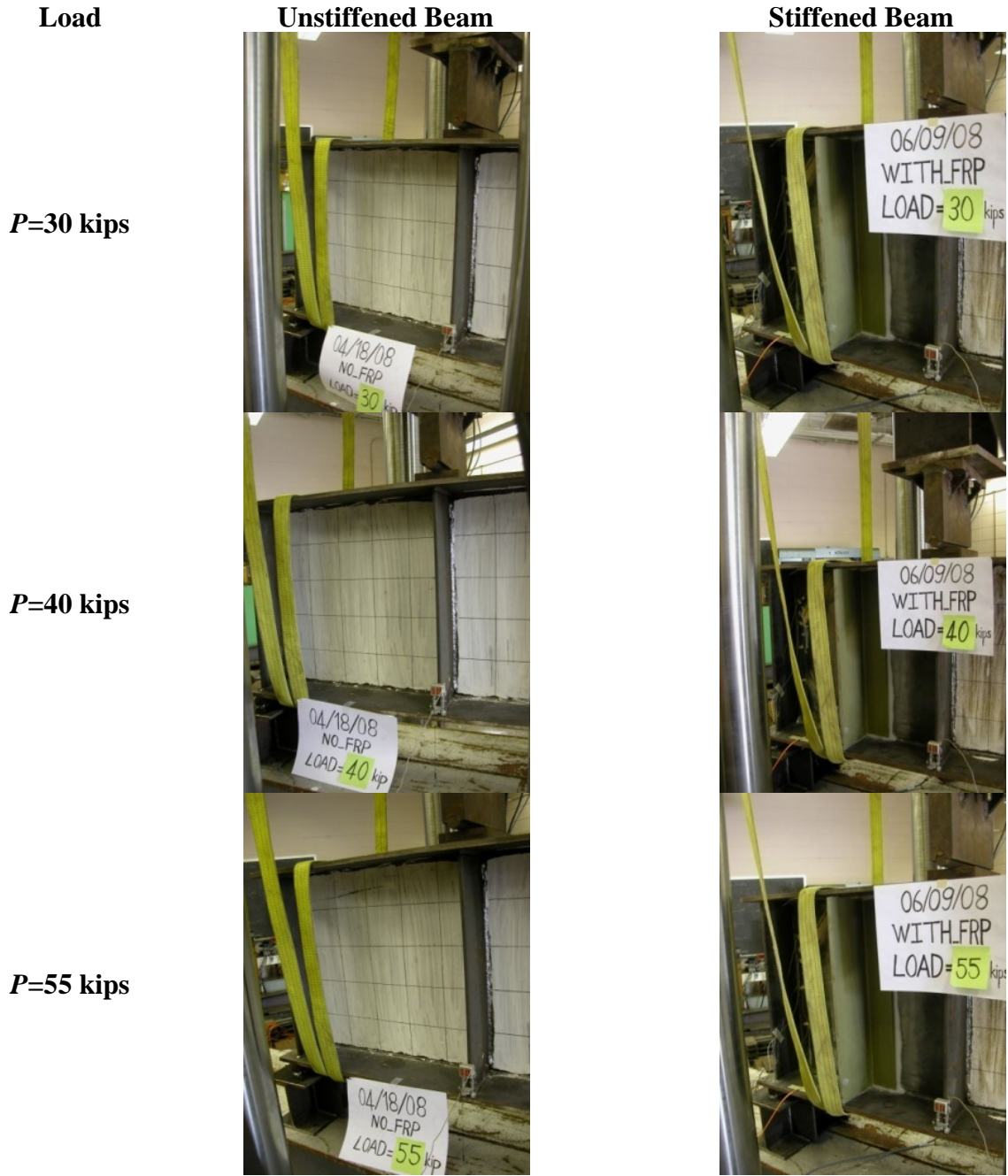


**Figure 16**  
**Progression of loading for beam specimens**

**Beams**

**Unstiffened**

**Stiffened**

**$P=60$  kips**



**$P=65$  kips**

**Failed**



**$P=75$  kips**

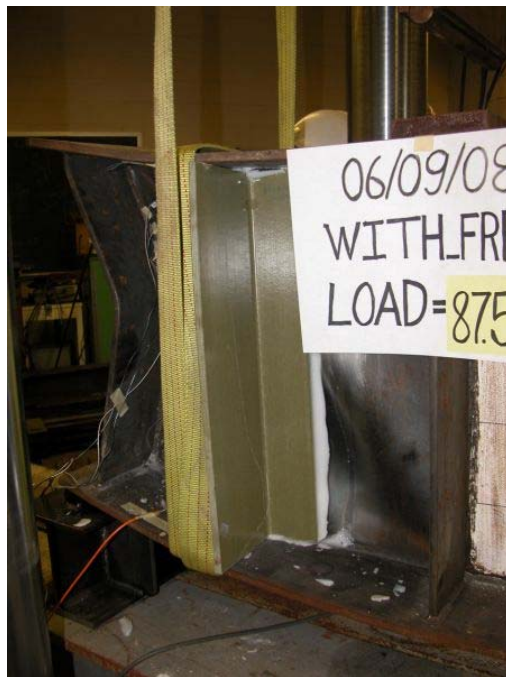
**Failed**



**Figure 16**  
**Progression of loading for beam specimens (continued)**



(a) Unstiffened specimen



(b) Stiffened specimen

Figure 17

Failure of beam specimens

Not only did the GFRP stiffener enhance the beam's strength, its load deflection ( $P - \Delta$ ) curve also improved when compared with the unstiffened specimen. Figure 18 is a plot of the normalized load deflection curve for both beam specimens. Both curves were normalized by

the results from the unstiffened beam (elastic deformation limit,  $\Delta_{el}$ , and failure load,  $P_f$ ). It can be seen that the GFRP-stiffened beam is demonstrating a stiffer response from the initiation of loading. The slope of the  $P - \Delta$  curve within the elastic range is about 17 percent higher than that of the unstiffened specimen. This modest increase in the stiffness of the stiffened beam does not justify the use of the proposed strengthening technique. The two GFRP stiffeners have an axial rigidity that is substantially higher than the bare steel web. This means that the in-plane contribution of the GFRP stiffener is limited as was the case for the axial tension specimen. The main contribution of the GFRP stiffener starts showing at higher loads. At the load level where the unstiffened beam buckled, it is clear that the stiffened beam is still behaving linearly. This linear behavior continues until a load equal to 72.5 kips ( $P/P_{f, \text{unstiffened}} = 1.16$ ). The plasticization of the web as indicated by the strain gage readings starts causing the  $P - \Delta$  relationship to become nonlinear. The following load step is when the initial epoxy cracking sound was heard, which kept increasing every load step thereafter until failure.

Studying the  $P - \Delta$  relationship from a ductility point of view shows that the increase in strength comes at considerable reduction in ductility, which is typical of FRP strengthening in general. Despite the reduction in ductility, the response of the stiffened beam is not perfectly brittle. The system is capable of absorbing a considerable amount of inelastic energy. Table 4 lists the ductility estimates for the stiffened and the unstiffened specimens calculated using two methods. The first ductility measure is based on the ratio of the deformation at failure to the deformation at the proportional limit. Another ductility measure is computed using the ratio between the amount of inelastic energy that would be absorbed by the system up to failure,  $E_{in}$ , to the total energy absorbed by the system,  $E_{total}$ . The inelastic energy is computed as the difference between the total energy,  $E_{total}$ , and the elastic energy,  $E_{el}$ , that would be released by the system if it were to be unloaded just before failure (shaded area in Figure 18). This ductility measure was used by Grace et al. and Okeil in studying FRP-strengthened concrete structures [25] and [26]. The deformation ductility for the stiffened beam is equal to 2.04 which is lower than the 4.44 value computed for the unstiffened specimen. Similar results were obtained for the energy ductility, which was computed to be 60.2 percent for the stiffened case compared to 85.8 percent for the unstiffened case. Nevertheless, both methods show that the stiffened beam specimen is not perfectly brittle, which corresponds to a deformation ductility factor of 1.0 or an energy ductility ratio equal to 0 percent.

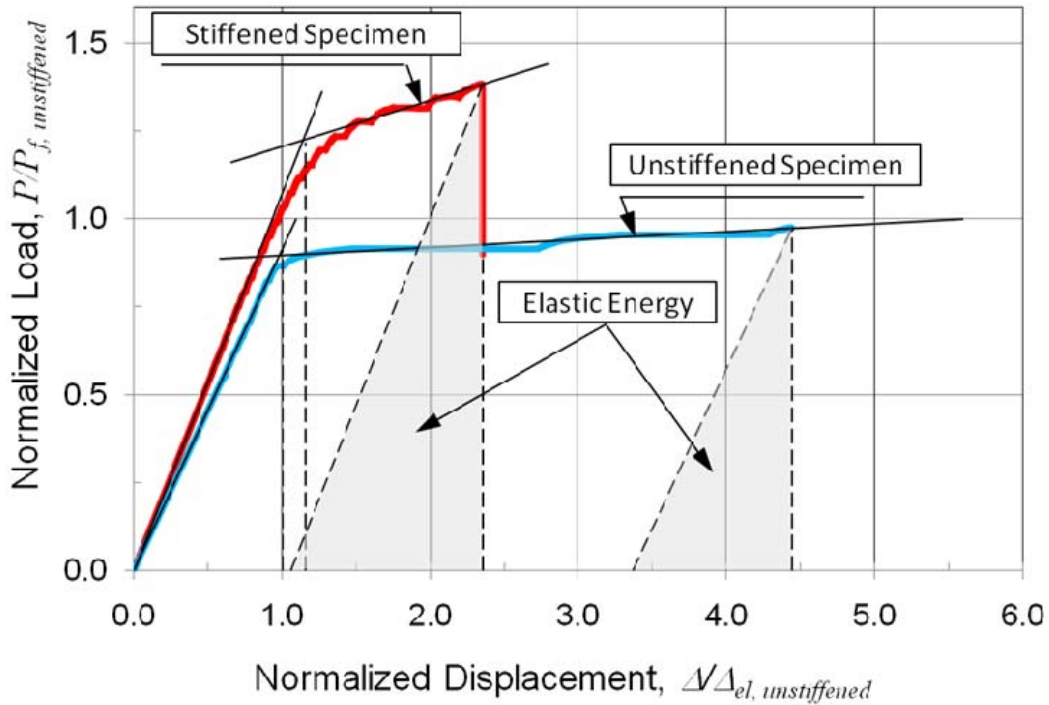


**Figure 18**  
**Comparison between the behavior of stiffened and unstiffened beam specimens**

**Table 4**  
**Ductility estimates for beam specimen**

Deformation Ductility		Energy Ductility (%)	
Unstiffened	Stiffened	Unstiffened	Stiffened
4.44	2.04	85.8	60.2

In summary, it can be said that the proposed technique is capable of improving the performance of buckling prone steel members by delaying the initiation of buckling, hence altering the mode of failure. This performance opens the door for a whole set of new FRP applications in strengthening of thin-walled steel structures. Moreover, this study reveals that the proposed technique does not require costly high modulus FRPs and high end epoxies. While these material choices would probably perform better, the proposed approach relies on improving the stiffness by using optimally oriented geometric sections to compensate for the low modulus material properties. The research is still at an early stage and more testing is needed to study various factors that may affect the performance of the proposed technique. Some of these factors will be discussed later in this report.

## Preliminary Analysis Results

### Eigen Buckling Analysis

Eigen buckling analyses were performed for both models to extract three mode shapes and mode frequencies. Figure 19, Figure 20, and Figure 21 present three mode shapes for the steel girder before and after the FRP strengthening.

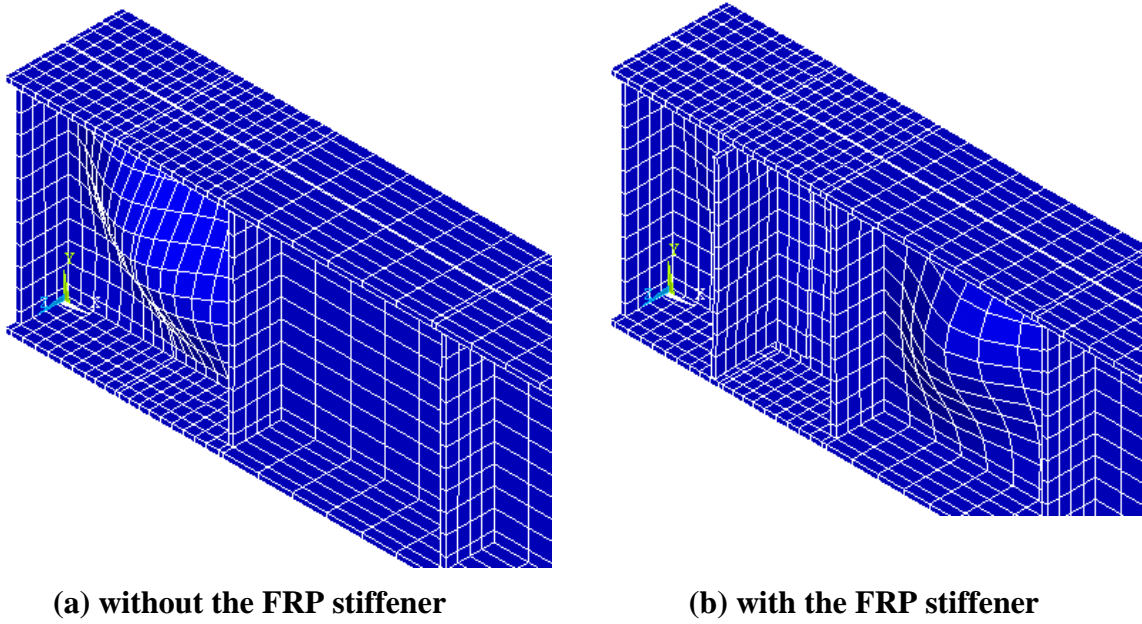
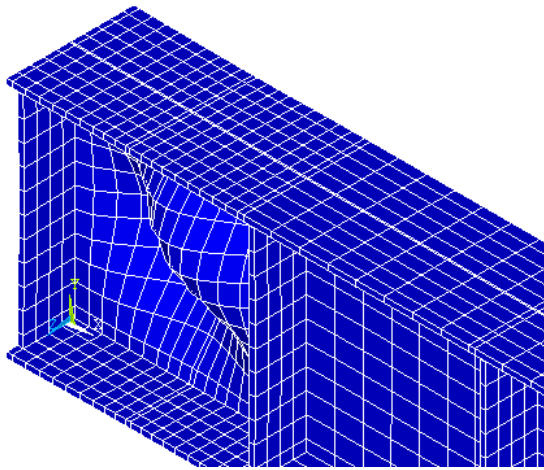
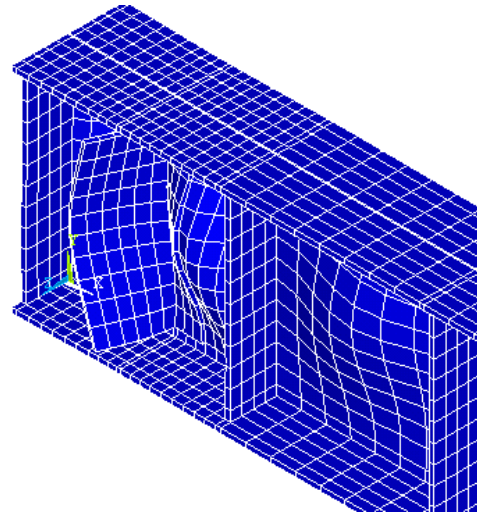


**Figure 19**  
**Deformed shape for first mode**

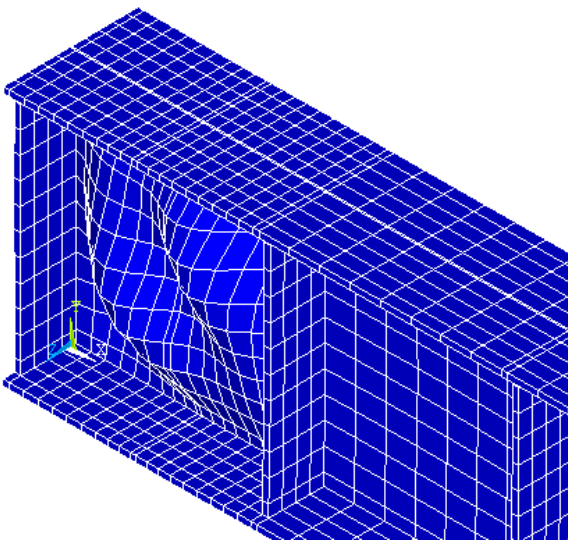


(a) without the FRP stiffener

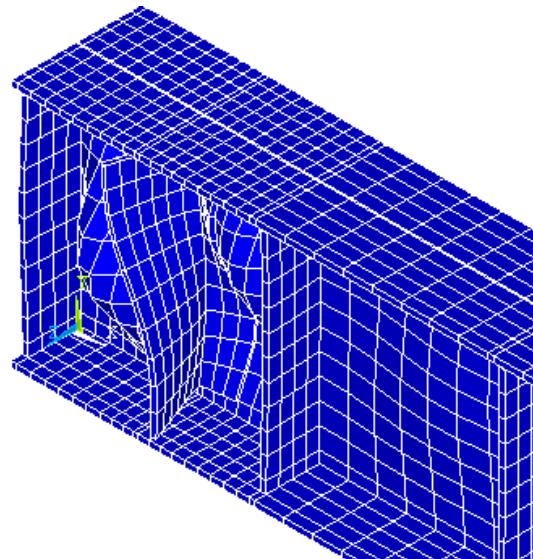


(b) with the FRP stiffener

**Figure 20**  
Deformed shape for second mode



(a) without the FRP stiffener



(b) with the FRP stiffener

**Figure 21**  
Deformed shape for third mode

Table 5 lists the eigenvalues corresponding to the first three modes for the girders with and without the FRP stiffener. Interpreting the eigenvalue results is done by using the resulting frequency of each mode as a multiplier to the applied load. For example, the frequency for the 1<sup>st</sup> mode of Model I is 0.741 for an assumed applied load equal to 100 kips. In that case, the eigen analysis predicts that an applied force equal to  $0.741 \times 100 \text{ kips} = 74.1 \text{ kips}$  is needed to initiate buckling.

**Table 5**  
**Mode frequencies for beam specimen (Applied Load,  $P = 100k$ )**

Model Type	Mode Number	Frequency
Steel Girder without the FRP stiffener	1	0.741
	2	0.860
	3	2.369
Steel Girder with the FRP stiffener	1	3.337
	2	3.392
	3	3.653

It is obvious from the shown modes that adding the FRP stiffener alters the mode shape, i.e., buckling mode. In the case of Mode 1, the unstiffened girder obviously suffers from a web buckling mode that takes place in the first panel subjected to high shear loads. After introducing the FRP stiffener, the first mode shape shows that the first panel is not the critical zone for buckling, but rather the buckling is shifted to the second panel that is unstiffened. Experimentally, the buckling took place in the first panel after debonding of the GFRP stiffener. The discrepancy behind these two different failure modes is due to the fact that the FE model still assumes perfect bond between the GFRP stiffener and steel plate. It is anticipated that by proper modeling of the mechanical characteristics of the epoxy adhesive, the proper mode of failure will be captured. Quantitatively, the expected buckling load multiplier for the first mode increases from 0.741 to 3.337 due to adding the FRP stiffener, which is again over predicting the buckling load (33.7 kips) due to the fact that the current model assumes a perfect bond between the FRP stiffener and the steel web and does not account for premature debonding. Therefore, the shown results do not take into account the delamination between the FRP and the steel that was observed experimentally.

### **Nonlinear Analysis**

Nonlinear Analyses were performed to study the feasibility of the FRP stiffener for strengthening steel girders. In the model, nonlinear material properties were considered for the steel elements, and large displacement analysis options were activated to consider nonlinear geometric conditions.

In real life, the steel girders experience straining actions due to the presence of partial loads before and during the installation of FRP stiffeners. This was reflected in the model by first applying 30 percent of the total load (load step 1) before activating the presence of FRP stiffeners. The auto time stepping options were activated to generate the sub steps based on the structural response for each load step. Figure 22 shows the load displacement curve for

Model I assuming two values of post-yield elastic modulus,  $E_p$ . It can be seen that an assumed  $E_p = 5$  percent of the initial elastic modulus of the steel,  $E_s$ , results in a flatter plateau which matches the behavior observed in the lab (see Figure 18). However, the buckling is initiated at a load equal to approximately 65 kips. Therefore, it was determined that the impact of different yield stress values be investigated. Figure 23 shows a plot of the same model for two yield stress values, namely the nominal value of 36 ksi, and an assumed value of 42 ksi. It should be noted that the actual yield stress of the web plate is yet to be tested, and that the material properties plotted in Figure 4 are for the axial tension specimen which is a different thickness (0.25 in. vs. 0.125 in.). Figure 24-a and b present the stress contours (S1) for both models just before the failure.

The final results for the stiffened beams that were included in the progress report are not included in this final report because the model is yet to account for failure of epoxy (debonding), which is the observed mode of failure experimentally. Thus, the model tends to overestimate the failure by a substantial margin. The resulting overestimation of the failure load is expected and is currently being addressed by modifying the FE model to account for epoxy debonding. The new model is highly nonlinear because of the brittle nature of the epoxy. Preliminary results show potential of accurately predicting the buckling behavior of the proposed strengthening scheme.

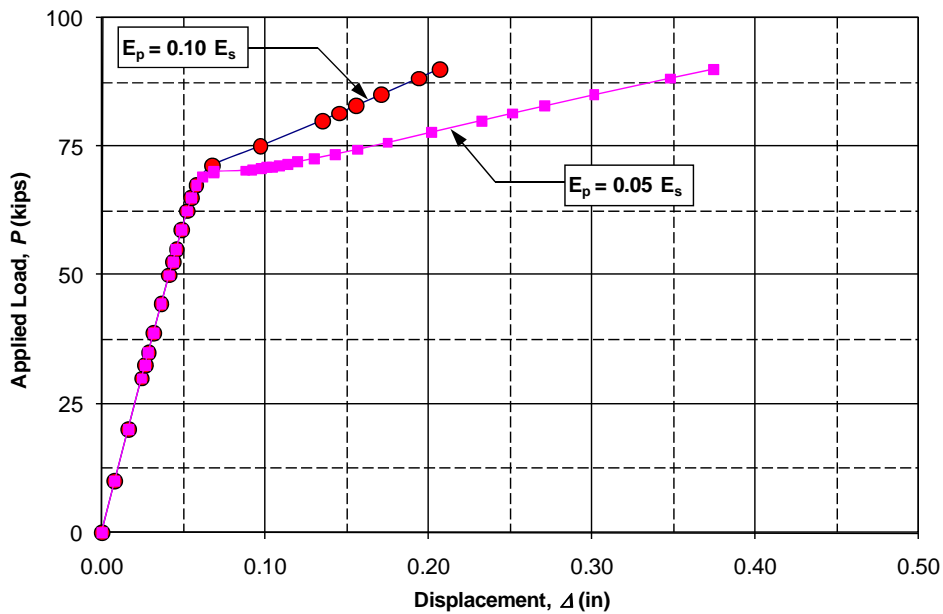


**Figure 22**  
**Sensitivity of load-displacement curve to post-yield modulus (Model I – without FRP)**

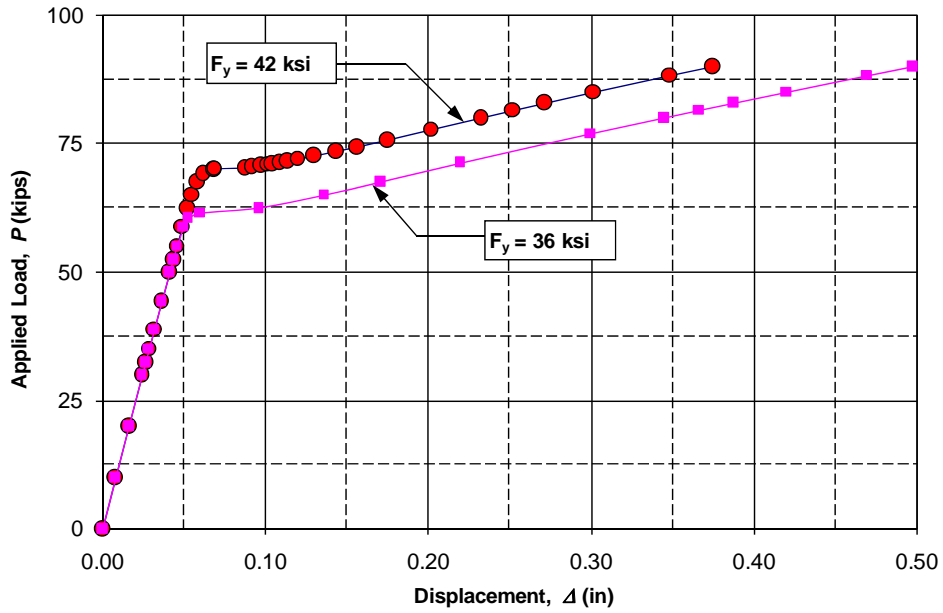


**Figure 23**  
Sensitivity of load-displacement curve to yield stress of steel (Model I – without FRP)

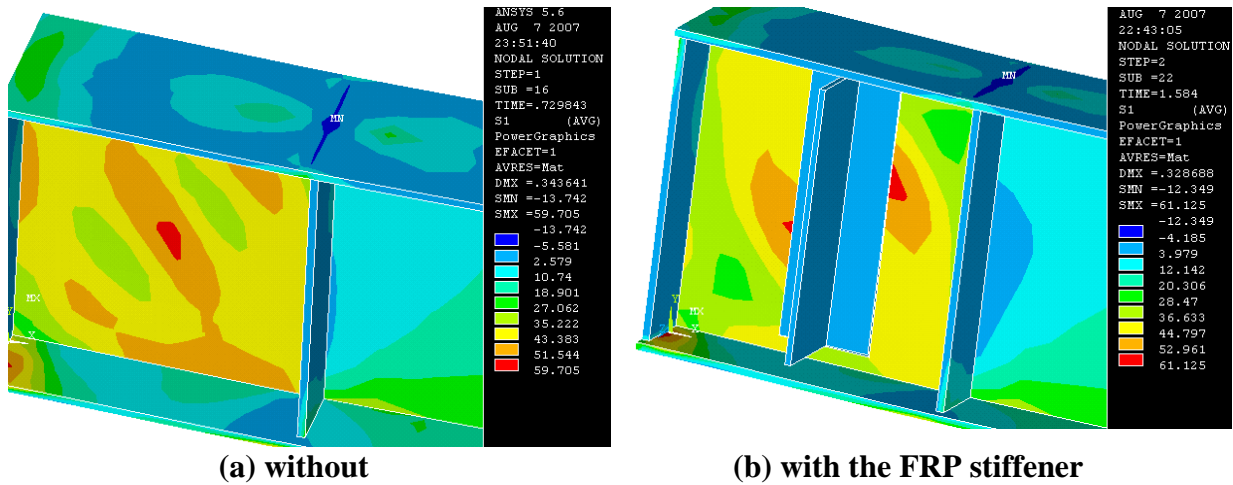


**Figure 24**  
Stress contours (S1) for models (a) without and (b) with the FRP stiffener just before failure



## CONCLUSIONS

The use of Glass Fiber Reinforced Polymer pultruded sections for strengthening steel structures was investigated. The GFRP section was bonded to thin-walled steel plates in an orientation that contributes to the out-of-plane stiffness of the plate more than the in-plane strength as is the common practice in most FRP strengthening applications. The two parameters contributing to the out-of-plane stiffness were the geometric and material properties of the GFRP stiffener. Because of the GFRP stiffener orientation, it is possible to use low modulus FRP materials rather than the more expensive high-modulus materials.

Two types of specimens were tested to demonstrate the difference in behavior between both strengthening techniques (in-plane and out-of-plane). Axial tension specimens were tested with and without GFRP sections bonded to the steel surface. This in-plane contribution was found to increase the stiffness of the tension specimen by 13 percent, which is a modest gain that may be beneficial for stiffening flexible structures that suffer from excessive deformations such as moveable bridges. Beam specimens were tested to explore the proposed out-of-plane strengthening technique. The results showed that stiffening the beam delayed web shear buckling (designed mode of failure) and that the failure load was 56 percent higher than the buckling load for the unstiffened beam. The behavior of the stiffened beam was ductile yet to a lesser extent than the unstiffened beam, which is common with most FRP strengthening techniques.

No code provisions exist for estimating the shear capacity of steel beams with FRP stiffeners. The existing code was still used to estimate the increase in strength assuming that the GFRP stiffener behaved in an identical manner as steel stiffeners. According to these calculations, the code estimated a 219 percent increase in strength. This substantially higher estimate was due to the fact that the debonding of the GFRP stiffener was not taken into account. Thus, it can be stated that new formulas will need to be developed for estimating the strength of GFRP-stiffened steel webs. This will require a concerted research effort to cover the various parameters that may affect the performance of the proposed technique such as: (1) the ratio between out-of-plane geometric and material properties of the GFRP stiffener and the bare steel member, (2) the contact area between the GFRP stiffener and the steel member, (3) the orientation of the GFRP stiffener, (4) mechanical properties of the epoxy used to bond the GFRP stiffener, (5) the impact of cycling loading on the performance of the strengthening technique, and (6) the original mode of failure of the unstiffened beam (i.e., full plasticization, inelastic buckling, and elastic buckling).



## RECOMMENDATIONS

Since this study was limited in scope, no specific implementation recommendation could be presented. Also, no code provisions exist for estimating the shear capacity of steel beams with FRP stiffeners. The existing code was still used to estimate the increase in strength assuming that the GFRP stiffener behaved in an identical manner as steel stiffeners. According to these calculations, the code estimated as 219 percent increase in strength. This substantially higher estimate was due to the fact that the debonding of the GFRP stiffener was not taken into account.

Thus, it can be stated that new formulas will need to be developed for estimating the strength of GFRP-stiffened steel webs. This will require a concerted research effort to cover the various parameters that may affect the performance of the proposed technique such as:

- the ratio between out-of-plane geometric and material properties of the GFRP stiffener and the bare steel member,
- the contact area between the GFRP stiffener and the steel member,
- the orientation of the GFRP stiffener,
- mechanical properties of the epoxy used to bond the GFRP stiffener,
- the impact of cycling loading on the performance of the strengthening technique, and
- the original mode of failure of the unstiffened beam (i.e., full plasticization, inelastic buckling, and elastic buckling).

Finally, the proposed stiffening technique may not limited to shear strengthening. The same approach can be used for any buckling prone member. For example, a compression flange may be stiffened in a similar manner by bonding a GFRP stiffener to its top or bottom surface. In other words, this study opens new venues for a wide range of new applications of FRP materials for structural strengthening.

Based on the findings from this study, the recommendations stemming out of this research are summarized next:

- (1) A full-fledged research project is needed to comprehensively investigate the various parameters that affect this strengthening technique. The new study should entail at least the following:

- a) conduct a comprehensive experimental program addressing the various parameters that this study has identified in addition to any other parameters that may also influence the behavior,
  - b) perform a thorough analytical investigation to assist in understanding the complex behavior of the strengthening technique,
  - c) develop simplified design tools based on the experimental and analytical investigations that can be used by engineers in everyday,
  - d) assess the feasibility of the proposed technique in comparison with alternative strengthening methods, and
  - e) identify deficient structures in the Louisiana bridge inventory that are suitable candidates to employ the new strengthening technique on a pilot basis.
- (2) The findings of the new study should be disseminated through a technology transfer workshop or short course by LTRC to DOTD engineers at TTEC.
- (3) Finally, it is recommended that a similar pilot study be conducted where FRP stiffeners are employed to inhibit buckling inducing modes of failure other than shear (e.g. compression flange buckling due to flexure).

## ACRONYMS, ABBREVIATIONS, & SYMBOLS

AASHTO	American Association of State Highway and Transportation Officials
ACI	American Concrete Institute
ASTM	American Society for Testing and Materials
$A, A_i, A_f$	cross sectional area (general, initial, and final)
$A_w$	cross sectional area of web
$b_f$	width of flange
$C$	Shear strength coefficient
CFRP	Carbon Fiber Reinforced Polymer
$D$	web depth
$d_o$	stiffener spacing
$E, E_i, E_p, E_f$	modulus of elasticity (general, initial, post-yield, and final)
$E_{el}, E_{in}, E_{total}$	energy (elastic, inelastic, and total)
FRP	Fiber Reinforced Polymer
$F_{cr}$	critical steel stress
$F_y, F_{yw}, F_{yf}$	yield stress of steel (general, web, and flange)
GFRP	Glass Fiber Reinforced Polymer
$I_x, I_y$	cross-sectional moment of inertia (about $x$ -axis and about $y$ -axis)
$L$	length of specimen
LTRC	Louisiana Transportation Research Center
$P, P_f$	applied load (general and at failure)
$P_n$	Nominal load capacity of stiffener
$r$	radius of gyration
$S_x$	cross-sectional modulus
$t_f$	thickness of flange
$t_w$	web thickness
$v, v_n$	shear flow (general and nominal)
$V_n, V_p$	shear strength (nominal and plastic)
$\varepsilon_s$	strain in steel
$\Delta, \Delta_{el}$	deformation (general and elastic limit)



## REFERENCES

1. Nanni, A. "Flexural behavior and design of RC members using FRP reinforcement," *Journal of Structural Engineering*, ASCE, Vol. 119, No. 11, 1993, pp. 3344-3359.
2. Khalifa, A.; Gold, W. J.; Nanni, A.; and Aziz, A. M. I. "Contribution of externally bonded FRP to shear capacity of RC flexural members," *Journal of Composites for Construction*, ASCE, Reston, VA, USA, Vol. 2, No. 4, 1998, pp. 195-202.
3. ACI Committee 440. "State-of-the-art report on fiber reinforced plastic (FRP) reinforcement for concrete structures." ACI 440R-96, American Concrete Institute, Farmington Hills, MI, 1996.
4. ACI Committee 440. "Guide for the Design and Construction of Externally Bonded FRP Systems for Strengthening Concrete Structures." ACI 440.2R-02, American Concrete Institute, Farmington Hills, MI, 2002.
5. CSA. "Design and Construction of Building Components with Fibre-Reinforced Polymers." S806-02, Canadian Standards Association, Rexdale, Ontario, 2002.
6. ACI Committee 440. "Guide for the Design and Construction of Concrete Reinforced with FRP Bars." ACI 440.1R-03, American Concrete Institute, Farmington Hills, MI, 2003.
7. Schnerch, D.; Stanford, K.; Sumner, E. A.; and Rizkalla, S. "Strengthening steel structures and bridges with high-modulus carbon fiber-reinforced polymers - Resin selection and scaled monopole behavior," *Transportation Research Record*, No. 1892, 2004, pp. 237-245.
8. Sen, R.; Liby, L.; and Mullins, G. "Strengthening steel bridge sections using CFRP laminates," *Composites Part B-Engineering*, Vol. 32, No. 4, 2001, pp. 309-322.
9. Vatovec, M.; Kelley, P. L.; Brainerd, M. L.; and Kivela, J. B. "Post strengthening of steel members with CFRP," 47th International SAMPE Symposium and Exhibition, May 12-16 2002, Soc. for the Advancement of Material and Process Engineering, Long Beach, CA, United States, Vol. 47 II, 2002, pp. 941-954.
10. Tavakkolizadeh, M. and Saadatmanesh, H. "Repair of damaged steel-concrete composite girders using carbon fiber-reinforced polymer sheets," *Journal of*

Composites for Construction, American Society of Civil Engineers, Reston, VA 20191-4400, United States, Vol. 7, No. 4, 2003, pp. 311-322.

11. Al-Saidy, A. H.; Klaiber, F. W.; and Wipf, T. J. "Repair of steel composite beams with carbon fiber-reinforced polymer plates," *Journal of Composites for Construction*, American Society of Civil Engineers, Reston, VA 20191-4400, United States, Vol. 8, No. 2, 2004, pp. 163-172.
12. Fawzia, S.; Al-Mahaidi, R.; Zhao, X. L.; and Rizkalla, S. "Strengthening of circular hollow steel tubular sections using high modulus CFRP sheets," *Construction and Building Materials*, Elsevier Ltd, Oxford, OX5 1GB, United Kingdom, Vol. 21, No. 4, 2007, pp. 839-845.
13. Shaat, A. and Fam, A. "Axial loading tests on short and long hollow structural steel columns retrofitted using carbon fibre reinforced polymers," *Canadian Journal of Civil Engineering*, Vol. 33, No. 4, 2006, pp. 458-470.
14. Moy, S. and Lillistone, D. "Strengthening cast iron using FRP composites," *Proceedings of the Institution of Civil Engineers: Structures and Buildings*, Thomas Telford Services Ltd, London, E14 4JD, United Kingdom, Vol. 159, No. 6, 2006, pp. 309-318.
15. Miller, T. C.; Chajes, M. J.; Mertz, D. R.; and Hastings, J. N. "Strengthening of a steel bridge girder using CFRP plates," *Journal of Bridge Engineering*, American Society of Civil Engineers, Vol. 6, No. 6, 2001, pp. 514-522.
16. Hollaway, L. C. and Cadei, C. "Progress in the technique of upgrading metallic structures with advanced polymer composites," *Progress in Structural Engineering and Materials*, Wiley Interscience, Vol. 4, No. 2, 2002, pp. 131-148.
17. Buyukozturk, O.; Gunes, O.; and Karaca, E. "Progress on understanding debonding problems in reinforced concrete and steel members strengthened using FRP composites," *Construction and Building Materials*, Elsevier Ltd, Vol. 18, No. 1, 2004, pp. 9-19.
18. Colombi, P. and Poggi, C. "Strengthening of tensile steel members and bolted joints using adhesively bonded CFRP plates," *Construction and Building Materials*, Elsevier Ltd, Oxford, OX5 1GB, United Kingdom, Vol. 20, No. 1-2, 2006, pp. 22-33.

19. Sebastian, W. and Luke, S. "Interface failure mechanics of elastically (advanced composite) reinforced steel members," *Journal of Structural Engineering*, American Society of Civil Engineers, Reston, VA 20191-4400, United States, Vol. 133, No. 5, 2007, pp. 683-694.
20. Schnerch, D.; Dawood, M.; Rizkalla, S.; and Sumner, E. "Proposed design guidelines for strengthening of steel bridges with FRP materials," *Construction and Building Materials*, Elsevier Ltd, Oxford, OX5 1GB, United Kingdom, Vol. 21, No. 5, 2007, pp. 1001-1010.
21. ASTM Standard E 8. "Standard Test Methods for Tension Testing of Metallic Materials," ASTM International, West Conshohocken, PA, Jan. 2008.
22. Strongwell Corporation. (2008) EXTREN® Series 500, "URL=[http://www.strongwell.com/products/pultruded\\_prod/struc\\_shapes/index.shtml](http://www.strongwell.com/products/pultruded_prod/struc_shapes/index.shtml), Date accessed=June 13, 2008."
23. Fyfe Co., LLC. (2008) Tyfo® S Epoxy, "URL=<http://www.fyfeco.com/products/epoxies.html>, Date accessed=June 13, 2008."
24. ANSYS. "Theory Reference," ANSYS, Inc., Canonsburg, PA, 2008.
25. Grace, N. F.; Soliman, A. K.; Abdel-Sayed, G.; and Saleh, K. R. "Behavior and ductility of simple and continuous FRP reinforced beams," *Journal of Composites for Construction*, ASCE, Reston, VA, USA, Vol. 2, No. 4, 1998, pp. 186-194.
26. Okeil, A. M. "Serviceability and ductility of PSC girders strengthened in flexure using CFRP laminates," 2003 ASCE/SEI Structures Congress and Exposition: Engineering Smarter, May 29-31 2003, American Society of Civil Engineers, Reston, VA 20191-4400, United States, Seattle, WA, United States, 2003, pp. 1215-1220.



## APPENDIX

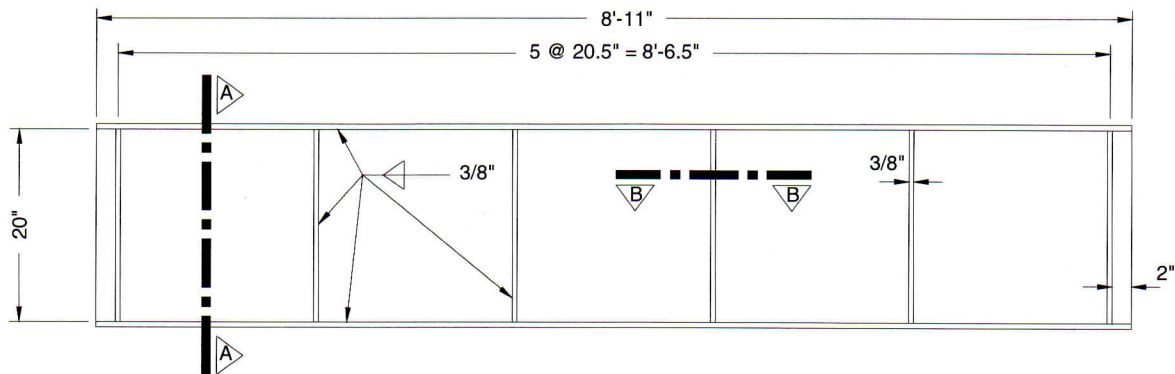


## Design Calculations – Unstrengthened Beam Specimen

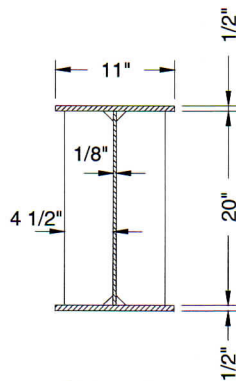
### Material Properties

A992 Steel ( $F_{yw} = 42 \text{ ksi}$ )

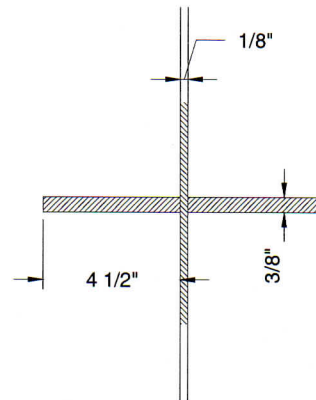
### Geometry



Elevation



Side View  
(Section A-A)



Stiffener Top View  
(Section B-B)

$$D = 20''$$

$$d_o = 20.5''$$

$$\frac{d_o}{D} = 1.025$$

$$t_w = \frac{1''}{8}$$

$$\frac{D}{t_w} = \frac{20''}{1/8''} = 160$$

web depth  
stiffener spacing

web thickness

$$\frac{h}{t_w} = 72 < 5.7 \sqrt{\frac{E}{F_y}} = 150$$

$$A_w = 1/8" \times 20" = 2.5 \text{ in}^2 \quad \text{area of web}$$

### Plate Girder Design

**Shear Design (End Panel).** The Plastic Shear Strength is given in Chapter 6 of AASHTO-LRFD (2004) as:

$$V_p = 0.58F_{yw}Dt_w = 60.9 \text{ kips}$$

The nominal shear resistance,  $V_n$ , is given as

$$V_n = V_p \left[ C + \frac{0.87(1-C)}{\sqrt{1+(d_o/D)^2}} \right]$$

for interior panels, and

$$V_n = CV_p$$

for end panels, which is the case for the beams tests. Therefore, the latter will be used in this study. First, the coefficient  $k$  is computed according to AASHTO-LRFD as

$$k = 5.0 + \frac{5.0}{(d_o/D)^2} = 9.759$$

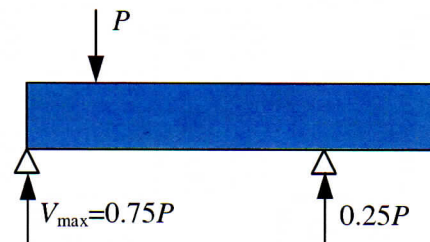
$$C = 1.0 \quad \text{for} \quad \frac{D}{t_w} = 160 \leq 1.12 \sqrt{\frac{Ek}{F_{yw}}} = 91.9 \quad \text{✗ N.G.}$$

$$C = \frac{1.12}{D/t_w} \sqrt{\frac{Ek}{F_{yw}}} = 0.575 \quad \text{for} \quad 1.12 \sqrt{\frac{Ek}{F_{yw}}} = 91.9 < \frac{D}{t_w} = 160 \leq 1.40 \sqrt{\frac{Ek}{F_{yw}}} = 114.9 \quad \text{✗ N.G.}$$

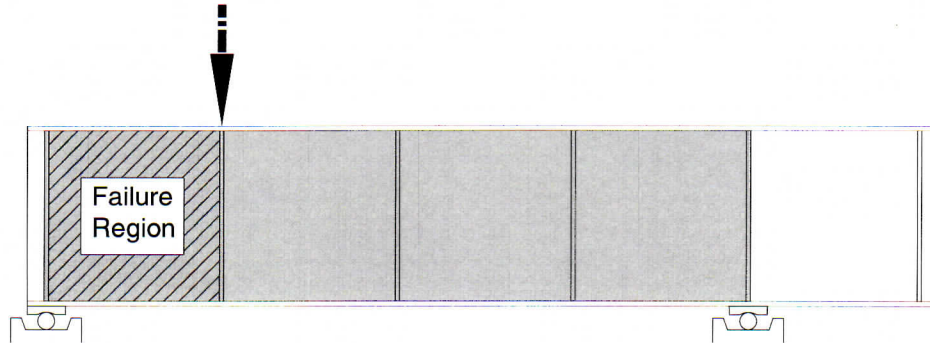
$$C = \frac{1.57}{(D/t_w)^2} \frac{Ek}{F_{yw}} = 0.413 \quad \text{for} \quad \frac{D}{t_w} = 160 > 1.40 \sqrt{\frac{Ek}{F_{yw}}} = 114.9 \quad \text{✓ O.K.}$$

$$V_n = CV_p = 25.8 \text{ kips}$$

$$\text{Applied Force, } P = \frac{V_n}{0.75} = 34.4 \text{ kips}$$



**Flexure Design.** The predicted failure load,  $P$ , is 35 kips. To ensure the elimination of the possibility of flexure mode of failure, the beam will be oversized in flexure to resist a much higher load than the predicted failure load.



$$\therefore M_P = 44.1 \text{ kip-ft}$$

$$\frac{D}{t_w} \leq 11.7 \sqrt{\frac{E}{F_{yw}}} = 307 \quad \checkmark \quad \text{O.K.}$$

Assuming a Flange Area,  $A_f$ , of  $1/2'' \times 11''$

$$\therefore A_f = 5.5 \text{ in}^2$$

$$\text{Total Area} = A_w + 2A_f = 13.5 \text{ in}^2$$

$$\text{Own Weight} = \left( \frac{13.5 \text{ in}^2}{144 \text{ in}^2/\text{ft}} \times 1 \text{ ft} \right) \times 490 \text{ lb/ft}^3 = 0.046 \text{ k/ft}$$

$$\therefore M_{OW} = 0.20 \text{ kip-ft}$$

$$\therefore M_u \cong M_P$$

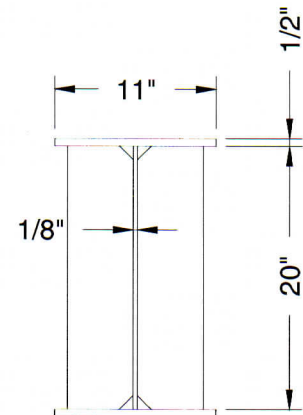
Say beam will be designed for

$$M_{\text{design}} = 300 \text{ kip-ft} \gg M_u$$

### Tension Field Check

$$I_x = \frac{11 \times 21^3}{12} - 2 \frac{5 \frac{7}{16} \times 20^3}{12} = 1239 \text{ in}^4$$

$$S_{xt} = \frac{I_x}{y_t} = \frac{1239}{10.5} = 118 \text{ in}^3$$



$$M_{nt} = S_{xt} R_e F_{yt} = 118 \times 1 \times 42 = 4956 \text{ lb-in} = 413 \text{ kip-ft}$$

where,

$$R_e = \frac{12 + a_r(3m - m^3)}{12 + 2a_r} = 1 \leq 1, \text{ and}$$

$$a_r = \frac{A_w}{A_f} = 0.82; \quad m = \frac{F_{yw}}{F_{yf}} = 1$$

$$M_{nt} \gg M_u$$

✓ O.K.

### Compression Field Check (Lateral Torsional Buckling)

$$I_y = \frac{1/2 \times 11^3}{12} + \frac{(1/6 \times 20) \times 7/16^3}{12} = 55.5 \text{ in}^4$$

$$A_T = \frac{1}{2} \times 11 + \frac{1}{6} \left( \frac{1}{8} \times 20 \right) = 5.92 \text{ in}^2$$

$$r_T = \sqrt{\frac{I_y}{A_T}} = 3.06 \text{ in}$$

$$\lambda = \frac{L_b}{r_T} = \frac{1.5 \times 6 \times 10/12}{3.06} = 40.2 < \lambda_p = 1.76 \sqrt{\frac{E}{F_{yf}}} = 46.3$$

$$\therefore F_{cr} = F_{yf} = 42 \text{ ksi}$$

### Compression Field Check (Flange Local Buckling)

$$\lambda = \frac{b_f}{2t_f} = \frac{11}{2 \times 1/2} = 11 > \lambda_p = 0.38 \sqrt{\frac{E}{F_{yf}}} = 10.0$$

$$\lambda = \frac{b_f}{2t_f} = \frac{11}{2 \times 1/2} = 11 < \lambda_r = 1.35 \sqrt{\frac{k_c E}{F_{yf}}} = 21.0$$

where,

$$k_c = \frac{4}{\sqrt{\frac{D}{t_w}}} = 0.316 \quad \text{use } k_{c, \min} = 0.35$$

∴ Failure will be by inelastic FLB and the critical stress is

$$F_{cr} = C_b F_{yf} \left[ 1 - 0.5 \left( \frac{\lambda - \lambda_p}{\lambda_r - \lambda_p} \right) \right] = 40.1 \text{ ksi}$$

where,

$$C_b = 1.0$$

$$R_{PG} = 1.0 \quad \text{for nonhybrid girders.}$$

$$M_{nc} = S_{xc} R_e R_{PG} F_{cr} = 4732 \text{ lb-in} = 394 \text{ kip-ft}$$

$$M_{nc} \gg M_u$$

✓ O.K.

### Bearing Stiffener Design

Assume  $t = 0.375''$  and  $b = 4.5''$

$$t = 0.375'' > 1.79 b \sqrt{\frac{F_y}{E}} = 0.306'' \quad \checkmark \text{ O.K.}$$

### Bearing Capacity:

$$A_{pb} = 2at = 2(4.5'' - 1.0'')0.375'' = 2.66 \text{ in}^2 \quad \text{assuming } 1'' \text{ weld size}$$

$$R_n = 1.8F_y A_{pb} = 201.1 \text{ kips} \gg P = 35 \text{ kips} \quad \checkmark \text{ O.K.}$$

### Compression Capacity – Intermediate Stiffener ( $d = 25 t_w$ ):

$$I = \frac{3.125 \times 1/8^3}{12} + 2 \left[ \frac{0.38 \times 4.5^3}{12} + (0.38 \times 4.5) \left( \frac{4.5 + 1/8}{2} \right)^2 \right] = 24.1 \text{ in}^4$$

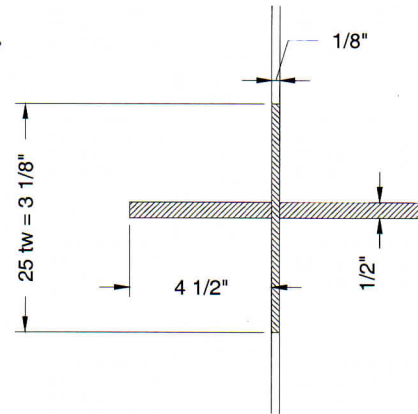
$$A = 3.125 \times \frac{1}{8} + 2 \times 4.5 \times 0.38 = 3.81 \text{ in}^2$$

$$r = \sqrt{\frac{I}{A}} = 2.52 \text{ in}$$

$$\frac{K L_b}{r} = \frac{0.75 \times 20''}{2.52''} = 5.95$$

$$\therefore F_{cr} = F_y = 42 \text{ ksi}$$

$$P_n = F_{cr} A = 160 \text{ kips} \gg P = 35 \text{ kips} \quad \checkmark \text{ O.K.}$$



**Compression Capacity – End stiffener ( $d = 12 t_w$ ):**

$$I = \frac{1.5 \times 1/8^3}{12} + 2 \left[ \frac{0.38 \times 4.5^3}{12} + (0.38 \times 4.5) \left( \frac{4.5 + 1/8}{2} \right)^2 \right] = 24.1 \text{ in}^4$$

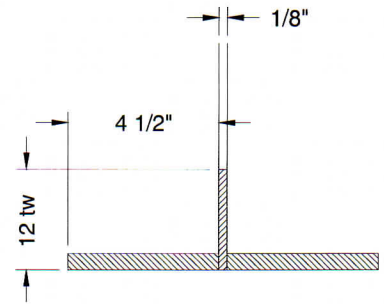
$$A = 1.5 \times \frac{1}{8} + 2 \times 4.5 \times 0.38 = 3.61 \text{ in}^2$$

$$r = \sqrt{\frac{I}{A}} = 2.58 \text{ in}$$

$$\frac{K L_b}{r} = \frac{0.75 \times 20''}{2.58''} = 5.81$$

$$\therefore F_{cr} = F_y = 42 \text{ ksi}$$

$$P_n = F_{cr} A = 151.6 \text{ kips} \gg 0.75P = 26.3 \text{ kips}$$



✓ O.K.

### Web Weld Design

$$V = 100 \text{ kips}$$

$$Q = 11" \times \frac{1}{2} \times \left( \frac{1}{2}(20") + \frac{1}{2}(1/2) \right) = 55.55 \text{ in}^3$$

$$I_x = 2 \left[ \frac{11 \times 1/2^3}{12} + (11 \times 1/2) \times 10 \frac{1}{4} \right] + \frac{1/8 \times 20^3}{12} = 1239.25 \text{ in}^4$$

$$v = \frac{VQ}{I} = \frac{100 \times 55.55}{1239.25} = 4.479 \text{ kip/in}$$

Assume weld thickness = 1/4"

$$R_r = 0.60\phi_{e2}F_{E70} = 0.60(0.80)70 = 33.60 \text{ ksi}$$

$$A_{eff} = 2 \times \frac{1/4}{\sqrt{2}} = 0.3536 \text{ in}^2$$

$$v_n = R_r A_{eff} = (33.60)(0.3536) = 11.88 \text{ kip/in} \gg v$$

✓ O.K.